Journal of Human Evolution 62 (2012) 225–241

Contents lists available at SciVerse ScienceDirect

Journal of Human Evolution

journal homepage: www.elsevier.com/locate/jhevol

A comprehensive morphometric analysis of the frontal and zygomatic bone of the Zuttiyeh fossil from Israel

S.E. Freidline [a,b,c,d,*], P. Gunz [a], I. Janković [e], K. Harvati [d,b,c], J.J. Hublin [a]

[a] Max Planck Institute for Evolutionary Anthropology, Department of Human Evolution, Deutscher Platz 6, Leipzig 04103, Germany
[b] Anthropology Ph.D. Program, City University of New York Graduate School, 365 Fifth Avenue, New York, NY 10016, USA
[c] New York Consortium in Evolutionary Primatology, NY, USA
[d] Institut für Ur- und Frühgeschichte, Eberhard Karls Universität Tübingen and Senckenberg Center for Human Evolution and Paleoecology, Rümelinstr, 23, 72070 Tübingen, Germany
[e] Institute for Anthropological Research, Gajeva 32, 10000 Zagreb, Croatia

ARTICLE INFO

Article history:
Received 5 January 2011
Accepted 8 November 2011

Keywords:
Homo heidelbergensis
Homo neanderthalensis
Middle Pleistocene
Israel
Semilandmark geometric morphometrics

ABSTRACT

The Zuttiyeh hominin craniofacial fossil was discovered in Israel in 1925. Radiometric dates and the archaeological context (Acheulo-Yabrudian) bracket the associated cave layers to between 200 and 500 ka (thousands of years ago), making it one of the earliest cranial fossils discovered in the Near East thus far. Its geographic position, at the corridor between Africa and Eurasia, in combination with its probable Middle Pleistocene date make it a crucial specimen for interpreting later human evolution. Since its discovery, qualitative descriptive and traditional morphometric methods have variously suggested affinities to *Homo erectus* (Zhoukoudian), *Homo neanderthalensis* (Tabun), and early *Homo sapiens* (Skhul and Qafzeh). To better determine the taxonomic affinities of the Zuttiyeh fossil, this study uses 3D semilandmark geometric morphometric techniques and multivariate statistical analyses to quantify the frontal and zygomatic region and compare it with other Middle to Late Pleistocene African and Eurasian hominins.

Our results show that the frontal and zygomatic morphology of Zuttiyeh is most similar to Shanidar 5, a Near East Neanderthal, Arago 21, a European Middle Pleistocene hominin, and Skhul 5, an early *H. sapiens*. The shape differences between archaic hominins (i.e., *Homo heidelbergensis* and *H. neanderthalensis*) in this anatomical region are very subtle.

We conclude that Zuttiyeh exhibits a generalized frontal and zygomatic morphology, possibly indicative of the population that gave rise to modern humans and Neanderthals. However, given that it most likely postdates the split between these two lineages, Zuttiyeh might also be an early representative of the Neanderthal lineage. Neanderthals largely retained this generalized overall morphology, whereas recent modern humans depart from this presumably ancestral morphology.

Introduction

The Zuttiyeh fossil human specimen (Turville-Pétre, 1927) was discovered in 1925 in Mugharat el Emireh (the Cave of the Robbers), near the Sea of Gallilee in Israel. It consists of a nearly complete frontal, right zygomatic and a partial right sphenoid bone and has been dated to the Middle Pleistocene period through correlation with the Tabun archaeological sequence. This sequence is central to understanding the chronology of Western Asia and is frequently used as a reference for interpreting archaeological cultures at other Pleistocene sites, such as Mugharet el Emireh, the Mount Carmel caves, Qafzeh and Kebara (Bar-Yosef, 1992). The Zuttiyeh craniofacial fragment was discovered at the base of the archaeological sequence at Mugharat el Emireh, under a layer that contained Acheulian-Yabrudian lithics, a pre-Mousterian technology similar to the Tabun E industry (Gisis and Bar-Yosef, 1974; Bar-Yosef, 1988).

Although there are no absolute dates from Mugharat el Emireh, Acheulo-Yabrudian layers have been radiometrically dated (thermoluminescence, electron spin resonance, and uranium series) from various sites in the Near East and range from >382 to 200 ka (thousands of years ago) (Yabrud Rockshelter 1: Huxtable, 1990; Bar-Yosef, 1992; Tabun: Mercier et al., 1995; Mercier and Valladas, 2003). Additionally, Tabun E, F, and G have been correlated with Isotope Stages 11–13, extending the age range of Acheulo-Yabrudian

* Corresponding author.
E-mail addresses: sarah.freidline@eva.mpg.de, sfreidline@gmail.com (S. E. Freidline), gunz@eva.mpg.de (P. Gunz), ivor.jankovic@inantro.hr (I. Janković), katerina.harvati@ifu.uni-tuebingen.de (K. Harvati), hublin@eva.mpg.de (J.J. Hublin).

0047-2484/$ – see front matter © 2011 Elsevier Ltd. All rights reserved.
doi:10.1016/j.jhevol.2011.11.005

to 400–500 ka. Therefore, the Zuttiyeh human fossil is most likely bracketed to between 500 and 200 ka.

Since its discovery, the taxonomic and phylogenetic interpretation of the Zuttiyeh fossil has been contentious (for a detailed review see Sohn and Wolpoff, 1993) and influenced by revised and improved dating of the West Asian fossil hominin record and individual and historic perspectives concerning the tempo and mode of later human evolution. At the time of its discovery, both the archaeological context of the fossil and the geological antiquity of the site were unclear. Many of the earliest studies incorporating the Zuttiyeh fossil identified morphological similarities to Neanderthals (Keith, 1927; Hrdlička, 1930; McCown and Keith, 1939; Weidenreich, 1943), however, the definition of Neanderthal varied among researchers. For example, Hrdlička (1930) suggested that the fossil showed a strong resemblance to the Asian Early Pleistocene Zhoukoudian E1 cranium, which he believed was a Neanderthal. McCown and Keith (1939) regarded Tabun 1 and Skhul 5 to be Neanderthals of the same population, with Zuttiyeh being more similar to Tabun 1. Weidenreich (1943) stressed its affinities to Skhul 5, which he considered to be an 'advanced Neanderthal' intermediate between more 'primitive Neanderthals', including Kabwe, Saccopastore, Steinheim, Tabun and Qafzeh, and anatomically modern humans. Additionally, Coon (1963) regarded Zuttiyeh as a possible descendant of a central European Neanderthal such as Krapina or Ehringsdorf. Suzuki and Takai (1970) concluded that Zuttiyeh's morphology was more archaic than the Amud male and most similar to Shanidar 1 and Tabun 1.

Once it became apparent that the Zuttiyeh fossil was actually older than many of the West Asian fossil hominins yet discovered, its interpretation as a Neanderthal relative became less common. Vandermeersch (1989) saw it as transitional between *Homo erectus* and the West Asian modern humans (e.g., Skhul and Qafzeh) with no special relationship to Neanderthals, while others (Smith et al., 1989; Trinkaus, 1989; Simmons et al., 1991) interpreted it as a generalized ancestor of all Late Pleistocene West Asian hominins (e.g., Amud, Tabun, Shanidar, Skhul and Qafzeh).

Sohn and Wolpoff (1993) concluded that Zuttiyeh neither expressed uniquely Neanderthal nor modern human features, but instead retained many features similar to those of East Asian hominins, being particularly similar to the early Middle Pleistocene specimens from Zhoukoudian (e.g., Zhoukoudian 11 and 12). They argued that Zuttiyeh provided a link between East and West Asian hominins, invalidating a unique African origin of modern humans around 200 ka or earlier. More recently, a cladistic analysis placed Zuttiyeh as a sister group to Skhul and these specimens as a sister group to modern humans, and concluded that it is the oldest known *Homo sapiens sapiens* (Zeitoun, 2001). Finally, Rightmire's (2009) craniofacial measurements grouped it in a paleo-community, or p-deme, within *Homo heidelbergensis* along with Bodo, Elandsfontein, Kabwe, Ndutu, Eyasi, and Omo 2.

Current opinion regarding the phylogenetic relationships between Middle to Late Pleistocene hominins in Western Asia can be divided into three general groups according to the perceived extent of admixture between archaic and modern humans in this region. One view supports complete admixture between the groups and a single species model (e.g., Frayer et al., 1993; Sohn and Wolpoff, 1993; Arensburg and Belfer-Cohen, 1998). Arensburg and Belfer-Cohen (1998) propose that there was regular gene flow between Africa and Asia and that the West Asian hominins represent a continuous chronological sequence from Zuttiyeh to *H. sapiens*. Correspondingly, Frayer et al. (1993) and Sohn and Wolpoff (1993) favor West Asian hominins as one species along with all post *Homo habilis* specimens, with an Asian rather than African origin. On the opposite end of the spectrum are those who recognize the presence of two species in the Near East: Neanderthals from Shanidar, Amud, Tabun (C1), Kebara (Units X and XII), and Dederiyeh, early *H. sapiens* from Skhul and Qafzeh (levels V-XXIV) and early Upper Paleolithic *H. sapiens* from Ksar Akil and Qafzeh (specimens 1 and 2) (e.g., Bar-Yosef, 1988, 1989; Vandermeersch, 1989). Supporters of this scenario recognize little to no admixture between archaic and modern humans. Lastly, some researchers (Smith, 1992; Trinkaus, 2005) advocate variable levels of admixture between African and Southwest Asian hominins. The assimilation model (Smith et al., 1989, 2005; Smith, 1992; Trinkaus, 2005) posits that anatomically modern humans emerged in Africa and migrated to Southwest Asia before migrating to southern Asia and higher latitude Eurasia. Rather than replacing the archaic populations they encountered in Eurasia, some level of genetic exchange occurred between the indigenous archaic and the migrating population.

Most recently, the sequencing of the complete Neanderthal genome revealed that between 1% and 4% of the genomes of people in Eurasia are likely derived from Neanderthals (Green et al., 2010). These authors conclude that low levels of interbreeding between archaic and modern humans most likely occurred in the Near East, when modern humans first left sub-Saharan Africa and before they expanded into Eurasia. However, these authors also suggest that ancient population substructuring within Africa could explain their results (see also Wall et al., 2009; Gunz et al., 2009a). Hodgson et al. (2010) propose a third scenario in which admixture occurred between Neanderthals and modern humans around 100 ka and then for climatic reasons modern humans retreated back to Africa, severing contact with Neanderthals. They argue that the presence of Neanderthal DNA in Europeans and Asians could be explained by founder effects during range expansion, and that traces of Neanderthal DNA may be present in unsampled modern Africa populations.

The geographic position of the Zuttiyeh fossil, in combination with its probable Middle Pleistocene age, makes it an interesting specimen for understanding aspects of later human evolution, including craniofacial morphological variability in Pleistocene human evolution and migration routes between Africa and Eurasia. Here we use three-dimensional geometric morphometric methods to quantify the frontal and zygomatic bone morphology of the Zuttiyeh fossil using landmarks and semilandmarks. We apply multivariate statistical analyses to identify which Pleistocene group it is most morphologically similar to: *H. erectus* s.l., *H. heidelbergensis* s.l., *Homo neanderthalensis*, transitional *H. sapiens*, early *H. sapiens*, Upper Paleolithic *H. sapiens* or recent *H. sapiens*. One of the major advantages of 3-D geometric morphometrics, and specifically curve and surface-semilandmarks, is that it allows researchers to quantify traits otherwise difficult to measure using traditional linear or even landmark-based geometric morphometrics (e.g., zygomatic orientation and browridge morphology; see Harvati, 2003b; Gunz and Harvati, 2007; Freidline et al., 2008, 2010; Harvati et al., 2010). Complex features can thus be quantified as continuous variables and included in multivariate statistical analyses.

Material and methods

Sample

This study includes a comprehensive sample of Early to Late Pleistocene fossil hominins and recent modern humans (Table 1). The fossil sample comprises all available Middle Pleistocene (780–128 ka) and West Asian specimens that preserve similar morphology to Zuttiyeh, as well as specimens that had been specifically compared with it in earlier studies. Additionally, some Early and Late Pleistocene fossils were included to provide a comparative framework. Table 1 lists the 34 fossils, their broad geographical origin, chronology and their attribution to taxonomic groups:

Table 1
Specimens, abbreviation (Ab.), chronology and classification used in the analysis. The classification was only used for the DFA analysis and to calculate group means (see text).

Specimen	Ab.	Chronology	Classification
Early Pleistocene: Africa			
KNM-ER 3733	ER3733	1.75 Ma (Feibel et al., 1989)	*H. erectus* s.l.
KNM-ER 3883	ER3883	1.50 Ma (Feibel et al., 1989)	*H. erectus* s.l.
Early Pleistocene: Asia			
Sangiran 17[a]	S17	1.50–1.02 Ma (Larick et al., 2001; Antón, 2003; Antón and Swisher, 2004)	*H. erectus* s.l.
Middle Pleistocene: Africa			
Bodo	Bd	ca. 600 ka (Clark et al., 1994)	*H. heidelbergensis* s.l.
Kabwe	Kb	700–400 ka (Klein, 1994)	*H. heidelbergensis* s.l.
Middle Pleistocene: Europe			
Arago 21[a]	Ar	600–350 ka (Cook et al., 1982; Falguères et al., 2004)	*H. heidelbergensis* s.l.
Petralona	Pt	670–ca. 250 ka (Harvati et al., 2009)	*H. heidelbergensis* s.l.
Sima de los Huesos 5[a]	Sm5	ca. 530 ka (Bischoff et al., 2007)	*H. heidelbergensis* s.l.
Middle Pleistocene: Asia			
Dali[a]	Dl	230–180 ka (Chen and Zhang, 1991)	*H. heidelbergensis* s.l.
Zhoukoudian 12 (E1)[a]	Z12	550–520 ka; ca. 580 ka; ca. 770 ka (Grün et al., 1997; Antón, 2003; Shen et al., 2009)	*H. erectus* s.l.
Zuttiyeh[a]	Zt	ca. 350, 500–200 ka (Huxtable, 1990; Bar-Yosef, 1992; Mercier et al., 1995; Mercier and Valladas, 2003)	Unclassified
Late middle-late Pleistocene: Africa			
Florisbad[a]	Fl	290–230 ka (Grün, 1996)	Unclassified
Jebel Irhoud 1	I1	ca. 160 ka (Smith et al., 2007)	Unclassified
Late middle-late Pleistocene: Europe			
Gibraltar 1	Gb1	71–50 to 35 ka (Klein, 1999)	*H. neanderthalensis*
Guattari	Gt	ca. 50 (Schwarcz et al., 1991)	*H. neanderthalensis*
Krapina 3	Kr3	140–120 ka (Rink and Schwarcz, 1995)	*H. neanderthalensis*
Krapina 6	Kr6	140–120 ka (Rink and Schwarcz, 1995)	*H. neanderthalensis*
La Chapelle-aux-Saints	LCh	56–47 ka (Grün and Stringer, 1991)	*H. neanderthalensis*
La Ferrassie 1	LF1	71–50 to 35 ka (Klein, 1999)	*H. neanderthalensis*
Late middle-late Pleistocene: Asia			
Amud 1[a]	Am1	ca. 50 ka (Rink et al., 2001)	*H. neanderthalensis*
Liujiang[a]	Ljg	139–111 ka (Shen et al., 2002)	Unclassified
Qafzeh 6	Q6	135–100 ka (Grün et al., 2005)	Unclassified
Shanidar 1[a]	Sh1	ca. 50 ka (Trinkaus, 1983)	*H. neanderthalensis*
Shanidar 5[a]	Sh5	ca. 50 ka (Trinkaus, 1983)	*H. neanderthalensis*
Skhul 5	Sk5	135–100 ka (Grün et al., 2005)	Unclassified
Upper Paleolithic Eurasian modern humans			
Brno 2[a]	Brn2	ca. 23 ka (Holt and Formicola, 2008)	Unclassified
Cro-Magnon 1	Cr1	28–27 ka (Holt and Formicola, 2008)	Unclassified
Mladeč 1	Ml1	ca. 31 ka (Holt and Formicola, 2008)	Unclassified
Předmostí 3[a]	Pr3	Early Upper Paleolithic (Smith, 1982)	Unclassified
Předmostí 4[a]	Pr4	Early Upper Paleolithic (Smith, 1982)	Unclassified
Oberkassel 1	Ob1	ca. 12 ka (Street, 2002)	Unclassified
Oberkassel 2	Ob2	ca. 12 ka (Street, 2002)	Unclassified
Zhoukoudian 101[a]	Zh101	ca. 13–33 (Chen et al., 1989; Hedges et al., 1992; Brown, 1992)	Unclassified
Zhoukoudian 102[a]	Zh102	ca. 13–33 (Chen et al., 1989; Hedges et al., 1992; Brown, 1992)	Unclassified
Recent modern humans			
Africa ($n = 44$): Egypt (5); South Africa (34); Tanzania (5)			*H. sapiens*
Asia ($n = 10$): Mongolia (5); Thailand (5)			*H. sapiens*
Australia ($n = 10$)			*H. sapiens*
Europe ($n = 58$): Austria (50); Belgium (2); Czech Republic (6)			*H. sapiens*
North America ($n = 108$): United States (100); Mexico (8)			*H. sapiens*
South America ($n = 5$): Argentina			*H. sapiens*

[a] Casts.

H. erectus s.l. ($N = 4$), *H. heidelbergensis* s.l. ($N = 6$), *H. neanderthalensis* ($N = 9$) and *H. sapiens* ($N = 235$). Although we recognize the taxonomy of the Early and Middle Pleistocene groups as controversial, these divisions have been supported in various studies (e.g., *H. erectus* s.l.: Rightmire, 1998a, 1998b; Asfaw et al., 2002; Antón, 2002, 2003; Potts et al., 2004; Baab, 2008; *H heidelbergensis* s.l.: Stringer, 1983; 2008; Harvati, 2009; Harvati et al., 2010). These prior group designations affect the mean shape calculations and the discriminant function analysis, but not the principal component analysis nor the nearest neighbor computations (see below).

The modern human sample ($N = 235$) is composed of 13 geographic populations spanning six continents: Australia (South

Australian Aborigines), Asia (Mongolia and Thailand), Europe (Austria and Czech Republic), Africa (Khoe-San, Egypt and Tanzania), North America (Arizona, Utah, Alaska and Mexico) and South America (Argentina). All modern human specimens are from the American Museum of Natural History (AMNH, New York) and from the South African Museum (Cape Town). Only adult crania were included (according to spheno-occipital fusion and eruption of permanent dentition) and individuals were sexed according to Howells (1973) criteria. When possible, an equal number of males and females were included.

Measurement protocol

Computed tomography (CT) and surface scans Landmarks were digitized on the extracted three-dimensional surface models from either surface scans or CT scans. CT scans were made with either an industrial CT scanner (BIR ACTIS 225/300) or a medical CT scanner (Toshiba Aquilion). The pixel size ranged from 0.24 to 0.49 mm and the slice thickness was between 0.25 and 1.00 mm. Surface scans of the remaining specimens were made with either a Minolta Vivid 910, capable of scanning a resolution of ~30 microns in the z plane, or a Breuckmann optoTOP-HE, with a resolution of ~6 microns in the z plane. Despite the differences in resolution between the surface scans and CT scans, all scans were of high enough resolution to not affect the ability to accurately digitize. If CT or surface scan data of the original fossil material were not available, surface scans of high quality casts from the Division of Anthropology of the AMNH (New York) or the Max Planck Institute for Evolutionary Anthropology (Leipzig) were made (see Table 1). After specimens were surface scanned, they were processed using either Geomagic Studio or OptoCat (Breuckmann) software, depending on the surface scanner used. For the CT data, three-dimensional surface models were extracted using Avizo (Visualization Sciences Group Inc.) and landmarks on these surfaces were then digitized using Landmark Editor (Wiley et al., 2005).

Landmark data The metric data set was designed to include all of the preserved morphology in the Zuttiyeh specimen. To quantify information on curves and surfaces, we used the method of semilandmarks (Bookstein, 1997; Gunz et al., 2005, 2009a,b) in addition to traditional landmark coordinates. The notion of homology employed here is one of geometric correspondence across a sample. 3D coordinates of landmarks (Table 2) and curve-semilandmarks were digitized on all specimens by one observer (S.F.). Techniques for surfaces differ substantially from those for curves in that, except for planes and cylinders, there is no straightforward way to distribute the semilandmarks. A mesh of surface-semilandmarks was digitized on one 'template' individual, comprising three surface patches (see Figure 1): one on the complete frontal bone and one on each zygomatic (the right zygomatic was reflected, see section on Data Reconstruction below), and a series of curves and biological landmarks (totaling 291 landmarks and semilandmarks). This template mesh of surface-semilandmarks was warped into the vicinity of every specimen according to the landmark and curve data using a thin-plate spline (TPS) interpolation between the template individual and each specimen in turn (Gunz et al., 2005). We then projected these warped points onto the surfaces by picking the closest vertices from the specimen's triangulated surface file. This protocol guarantees that every specimen has the same number of curve-semilandmarks and surface-semilandmarks in approximately corresponding locations. A detailed description can be found in Gunz et al. (2005, 2009a,b). To remove the confounding effects of the arbitrary spacing, these semilandmarks are then allowed to slide along the curves and surfaces prior to the statistical analysis. To linearize the minimization problem, the semilandmarks do not slide on the actual curve or surface but along the tangent vectors to the curve or the tangent planes to the surface. The initially equidistant semilandmarks were slid along tangents to the curves and tangent planes to the surfaces so as to minimize the bending energy of the TPS interpolation between each specimen and the Procrustes consensus configuration. After the sliding step, landmarks and semilandmarks can be treated the same in the subsequent multivariate analysis.

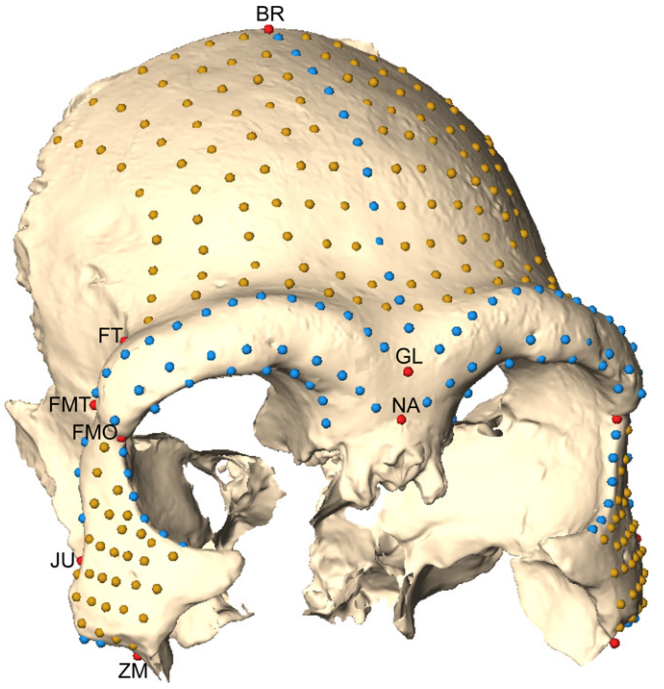

Figure 1. 291 Landmarks and semilandmarks digitized on all specimens, red: biological landmarks; blue: curve-semilandmarks; yellow: surface-semilandmarks. Biological landmarks are abbreviated. The full names are listed in Table 2. (For interpretation of the references to colour in this figure legend, the reader is referred to the web version of this article).

Table 2
Biological landmarks used in the analysis.

Landmark	Abbreviation
Bregma	BR
Glabella	GL
Frontomalare orbitale	FMO
Frontomalare temporale	FMT
Frontotemporale	FT
Jugale	JU
Nasion	NA
Zygomaxillare	ZM

A generalized Procrustes analysis (GPA) was used to superimpose a set of specimen landmark/semilandmark configurations onto the mean (consensus) configuration according to a least-squares criterion. GPA removes the effects of translation and rotation in the raw coordinate data and standardizes each specimen to unit centroid size – the square root of the sum of squared distances from each landmark to the specimen's centroid (Dryden and Mardia, 1998). All data processing and statistical analyses were performed in Mathematica (Wolfram Research) and R (R Development Core Team, 2010).

Missing data reconstruction Vandermeersch (1981, 1989) noted that Zuttiyeh's supraorbital torus was divided into medial and lateral components like in modern humans, especially on the

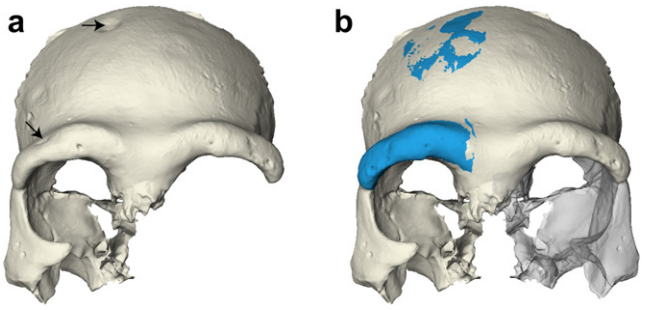

Figure 2. Virtual reconstruction of the Zuttiyeh fossil: a) the original cast of Zuttiyeh, which includes two pathologies indicated by the arrows, a possible deformation on the right browridge and a depression on the right posterior frontal bone; b) the virtual reconstruction that was measured and used in the analyses. The left browridge was mirror-imaged and merged onto the right frontal bone indicated in blue, some of the left posterior frontal was mirror-imaged and merged onto the right posterior frontal indicated in blue, and the entire right zygomatic was mirror-imaged and merged onto the left frontal in correct anatomical orientation indicated in transparent gray. (For interpretation of the references to colour in this figure legend, the reader is referred to the web version of this article).

right side. However, Simmons and her co-authors (1991) argued that the depression on the right side of the torus is a pathological lesion and does not represent a modern human-like biological separation of the browridge into two components. In order to correct for this possible pathology, we reflected the non-pathological left browridge and merged it to the existing right frontal bone (see Figure 2). Additionally, a large depression is present on the right side of the posterior frontal bone. We repaired this by mirror-imaging aspects of the left posterior frontal bone and merged it to the right frontal bone. Lastly, we reflected the entire right zygomatic bone and merged it to the existing frontal bone creating a complete left zygomatic bone in correct anatomical orientation. Figure 2 compares the original cast of Zuttiyeh (Figure 2a) with our reconstruction (Figure 2b).

We optimized our data set so as to include all relevant fossil specimens that preserved the morphology present on Zuttiyeh. As geometric morphometric methods require all specimens to have the same number of homologous points, some minor data reconstruction was necessary for some fossil specimens. If pieces of the frontal and/or zygomatic bone were missing or deformed, bilateral symmetry was exploited. In these cases, the scans of the specimens were mirrored along the midsagittal plane using the software Geomagic Studio and Avizo and then both sides were digitized. The following specimens were reflected: Bodo, Cro-Magnon 1, Dali, Florisbad, Gibralter 1, Guattari, Kabwe, KNM-ER 3883, Krapina 3, Krapina 6, La Ferrassie 1, Oberkassel 1, Předmostí 4, Shanidar 1 and Zhoukoudian 12.

If missing data occurred on both sides of the specimen or along the midline, landmarks were estimated using 'geometric reconstruction' via TPS following Gunz et al. (2009b). A TPS interpolation function was used to map the missing landmarks/semilandmarks from the sample average onto the target during the semilandmark sliding step (Gunz, 2005; Gunz and Harvati, 2007; Gunz et al., 2009a,b; Grine et al., 2010; Harvati et al., 2010; Gunz et al., 2011; Stansfield and Gunz, 2011). When a landmark or semilandmark is declared missing, it is 'fully relaxed' so as to minimize the overall bending energy between the incomplete specimen and the sample Procrustes average (Gunz et al., 2009b). Minimal reconstruction occurred primarily around the inferior border and/or posterior temporal process of the zygomatic bone (Bodo, Florisbad, Jebel Irhoud 1, Krapina 3, Krapina 6, Předmostí 4, Shanidar 5, Zhoukoudian 12 and Zuttiyeh), medial (KNM-ER 3733 and Jebel Qafzeh 6) and lateral (KNM-ER 3733 and Sima de los Huesos 5) browridge and aspects of the frontal bone (Jebel Irhoud 1, KNM-ER 3733, Krapina 3, La Chapelle-aux-Saints, Qafzeh 6 and Zhoukoudian 12).

Arago 21 was the most heavily reconstructed fossil (see Supplementary Figure 1). The whole face of Arago 21 (de Lumley and de Lumley, 1971), including the midline, is deformed by what appears to be an almost uniform shear. We used the virtual reconstruction of the specimen described in Gunz et al. (2009b). A cast of the face of Arago 21 was scanned with a high-resolution optical surface scanner (the cast was of a manual reconstruction and had already corrected for a local plastic deformation on the frontal bone of the original specimen). We measured points along the midsagittal curve and bilateral landmarks and used a method described in Gunz et al. (2009b) to remove the effects of the taphonomic distortion via reflected relabeling (Mardia et al., 2000; Bookstein, 2005). We reflected the landmarks measured on the cast across the *x*-axis (Supplementary Figure 1) and then interchanged the corresponding left and right labels of the bilateral points. After a least-squares superimposition of the original landmarks and the reflected relabeled landmarks, we computed their Procrustes mean shape, thereby creating a perfectly symmetric form (Mardia et al., 2000). We then computed a TPS interpolation between the original landmark coordinates and the symmetrized configuration and used it to warp the vertices of the triangulated surface.

Analyses A principal component analysis (PCA) of all 291 landmarks and semilandmark shape coordinates was performed in order to examine the overall shape variation in the frontal and zygomatic bone and the distribution of each group in shape space. A PCA reduces the dimensionality of high dimensional shape space (Bookstein, 1991; Rohlf, 1993) and provides summaries of large-scale trends within the data. To visualize the shape changes along the first two principal components (PCs), we used thin-plate spline warping of the Procrustes mean shape (see Gunz and Harvati, 2007; Mitteroecker and Gunz, 2009). A PCA was also performed in form space (Mitteroecker et al., 2004; Mitteroecker and Gunz, 2009). Form space included the log centroid size of each individual and is valuable because the relationship between shape and size can be explored. To determine which individuals are most similar in shape to Zuttiyeh, nearest neighbors in shape space were calculated using Procrustes distances. The Procrustes distance is the square root of the sum of squared differences of corresponding landmark coordinates in two Procrustes-superimposed figures (Slice, 2005). In order to estimate the range of variation within each taxonomic group (see Table 1 for groupings) and to provide a context for the individual distances between Zuttiyeh and its nearest neighbors, Procrustes distances were calculated between all possible pairs of individuals within each group.

A discriminant function analysis (DFA) was computed to assess how well the frontal and zygomatic bone morphology separates fossil and modern human groups. This analysis has been applied in previous studies to classify fossil specimens (e.g., Harvati, 2003a; Gunz and Harvati, 2007; Skinner et al., 2008; Glantz et al., 2009; Mounier et al., 2011; Stansfield and Gunz, 2011). DFA utilizes the space of canonical variates, which emphasizes among-group differences relative to within-group differences. The groups were defined a priori according to the population grouping shown in Table 1. Zuttiyeh as well as all transitional (Jebel Irhoud 1 and Florisbad), early (Skhul 5, Qafzeh 6 and Luijiang) and Upper Paleolithic *H. sapiens* were treated as individuals with unknown group affinities to be classified by posterior probabilities.

The computation of a DFA requires that the number of variables be smaller than the number of specimens. In order to reduce the

dimensionality of our data, we therefore used the subspace of the first few PCs of the Procrustes shape coordinates (see also below). A compromise has to be made between including enough variables (i.e., PCs) to provide a sufficient amount of shape information for discrimination, and using too many variables, thereby creating spurious clusters (for additional discussion of this issue see Skinner et al., 2008; Mitteroecker and Gunz, 2009; Mitteroecker and Bookstein, 2011). As the choice about how many PCs to use for the subspace is arbitrary, we computed our DFA multiple times using the first five to 16 PCs. In order to confirm that we did not choose too many PCs, we randomly relabeled all specimens so as to create false group compositions, and repeated the DFA. In this test, the DFA was not able to discriminate among these random groups, i.e., the clustering observed with the actual group labels in the subspace of the first few PCs was not an artifact of including too many variables.

Zuttiyeh was classified by posterior probability using four a priori groups: *H. erectus* s.l., *H. heidelbergensis* s.l., *H. neanderthalensis* and *H. sapiens* (Table 1). The transitional (Jebel Irhoud 1, Florisbad) and early anatomically modern human specimens (Qafzeh 6, Skhul 5 and Luijiang), and all Upper Paleolithic crania were also classified via posterior probability. Additionally, permutations tests (10,000 random permutations) using the Procrustes distances between the mean group shapes were performed to test for significant shape differences between groups.

To better illustrate the shape differences between Zuttiyeh, *H. erectus* s.l., *H. heidelbergensis* s.l., Neanderthals and modern humans, we generated Procrustes mean shapes for each of the aforementioned groups. We then used the semilandmark and landmark data set to warp the surface of Zuttiyeh to the mean of each group in Avizo.

Results

Principal component analysis

Procrustes shape space Figure 3 displays the first two PCs in shape space, which together account for 61.7% of total shape variation. Convex hulls are drawn for *H. erectus* s.l., *H. heidelbergensis* s.l., *H. neanderthalensis* and *H. sapiens*. The pattern in the first two PCs primarily reflects a contrast between archaic (all fossils excluding the Upper Paleolithic specimens) and modern human morphology. The Upper Paleolithic humans, except for Zhoukoudian Upper Cave 101 and 102, fall within the range of modern human variation. Zuttiyeh, as well as Jebel Irhoud 1 and Florisbad, cluster with the Neanderthals, Skhul 5 and Qafzeh 6 plot between the Neanderthals and modern humans, and Shanidar 5 falls within the range of modern human variation. *H. heidelbergensis* s.l. and *H. erectus* s.l. cluster separately from all other groups.

The shape changes along the PC axes are included in the PCA plot (see Figure 3a–d). PC 1 is primarily associated with the overall shape of the frontal bone and the robusticity of the browridge (Figure 3a and b). Individuals at the negative end of PC 1 have a low, receding frontal bone combined with a wide and projecting browridge. Among the fossils, the *H. erectus* s.l. and *H. heidelbergensis* s.l. specimens exhibit the most pronounced browridges and most receding frontal bones. This is especially true for Bodo and KNM-ER 3883, which plot at the extreme negative end of PC 1. Skhul 5, Qafzeh 6, Shanidar 5 and Zhoukoudian 101 and 102 are intermediate in this morphology between the more primitive *H. erectus* s.l./*H. heidelbergensis* s.l. and recent and Upper Paleolithic *H. sapiens*.

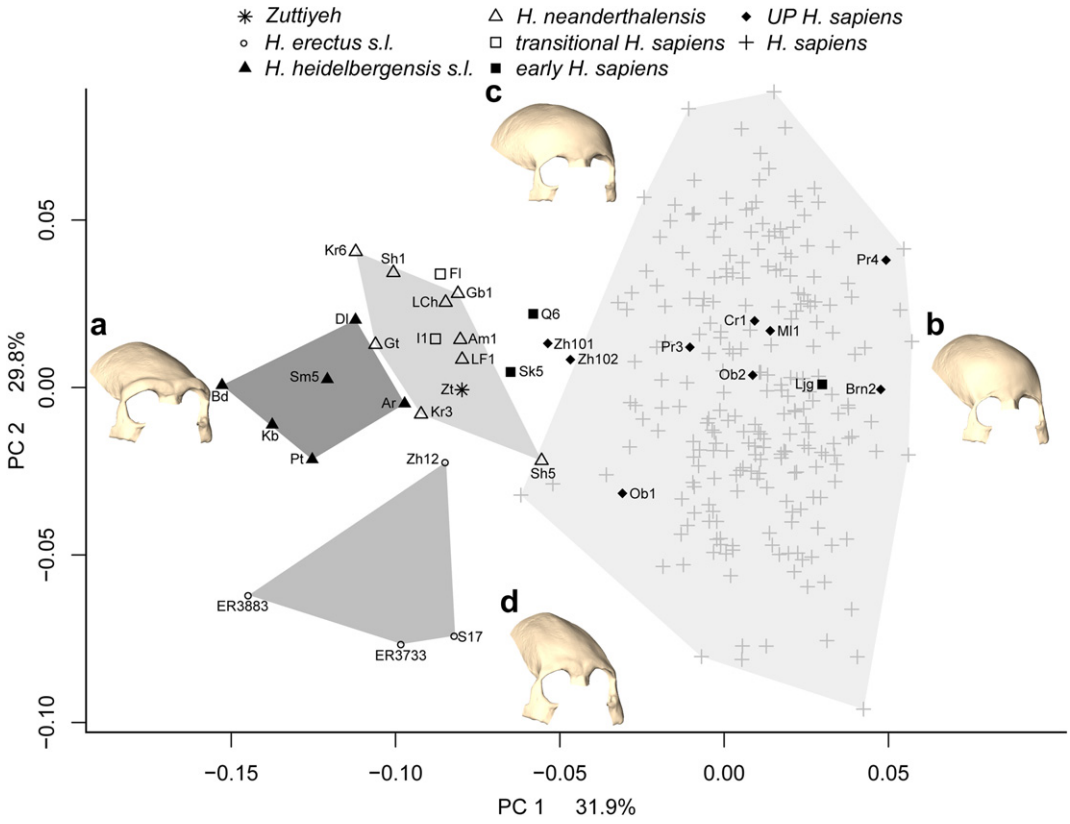

Figure 3. PCA in shape space. PC 1 represents 31.9% of total shape variation; PC 2 represents 29.8% of total shape variation. Convex hulls are drawn for *H. erectus* s.l., *H. heidelbergensis* s.l., *H. neanderthalensis* and recent *H. sapiens*; a) mean shape at the negative end of PC 1; b) mean shape at the positive end of PC 1; c) mean shape at the positive end of PC2; d) mean shape at the negative end of PC 2.

Along PC 2, the main shape changes are in frontal bone width and shape and zygomatic size (Figure 3c and d). Recent modern humans express more variability in these features than the fossil hominins. The European individuals have the widest and most rounded frontal bones plotting at the positive end of PC 2 (Figure 3c) and the North American populations exhibit narrower frontals, falling at the negative end of PC 2 (Figure 3d). Additionally the size and orientation of the zygomatic bone changes along PC 2. Individuals that plot at the negative end of PC 2 express much larger zygomatics that are angled more obliquely in the transverse plane. This angle is most apparent along the zygomaxillary arch and the medial section of the zygomatic bodies in Figure 3d.

We computed nearest neighbors based on inter-individual Procrustes distances and Zuttiyeh was most similar to Shanidar 5 (Procrustes distance: 0.051), a Near East Neanderthal, Arago 21 (0.061), a European Middle Pleistocene hominin included in the taxon *H. heidelbergensis* s.l., and Skhul 5 (0.063), an early anatomically modern human. Figure 4 plots the Procrustes distances between Zuttiyeh and its ten nearest neighbors in shape space, as well as the Procrustes distances between all possible pairs of individuals within each a priori group (*H. erectus* s.l., *H. heidelbergensis* s.l., *H. neanderthalensis*, *H. sapiens*). The distance between Zuttiyeh and Shanidar 5 is well below the median for each group. Except for the *H. erectus* s.l. median, the ranges and medians for each of the a priori groups are similar.

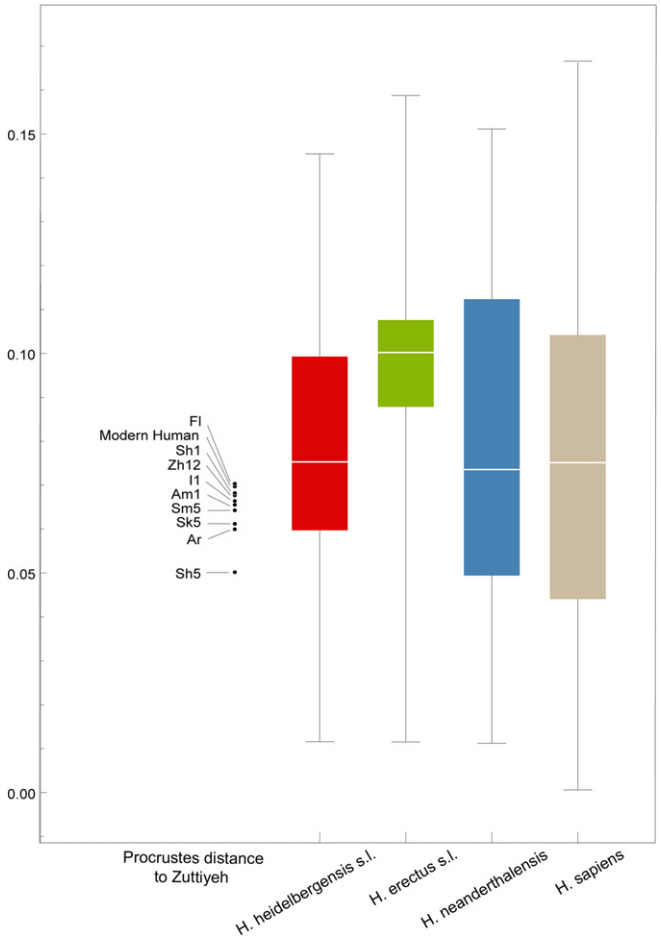

Figure 4. Procrustes distances between Zuttiyeh and its ten nearest neighbors in shape space and comparisons of intraspecific ranges of Procrustes distances for *H. erectus* s.l., *H. heidelbergensis* s.l., *H. neanderthalensis* and *H. sapiens*. The ranges were calculated by computing the Procrustes distances between all possible pairs within the a priori groupings shown in Table 1. The box plot illustrates the median value, first and third quartiles, and extreme values. Full names of the fossil specimens are listed in Table 1.

Procrustes form space PC 1 (Figures 5 and 6) in Procrustes form space (36.4% of total form variation) is highly correlated ($r \cong -0.94$) with log centroid size. Allometric trends (black lines in Figures 5 and 6) for *H. erectus* s.l., *H. heidelbergensis* s.l., *H. neanderthalensis*, and recent *H. sapiens* were computed by regressing shape on log centroid size. The Middle Pleistocene archaic humans, like Bodo, Petralona and Kabwe, exhibit the largest frontal and zygomatic bones. Like in the first principal component of shape space, PC 2 (21.1% of total form variation) in form space mainly illustrates a separation between modern and archaic humans. Zuttiyeh plots close to Zhoukoudian 12, its nearest neighbor in form space, along the *H. erectus* s.l. size trend and near the boundary of modern human variation (denoted by the convex hull). In Figure 6, we plotted PC 1 against PC 3 (17.0% of total form variation) in form space. In this dimension, Zuttiyeh appears closer to the *H. heidelbergensis* s.l. and Neanderthal allometric trends and within the range of modern human variation.

Discriminant function analysis

We performed a DFA (Figure 7), computed in the subspace of the first eight principal components of shape space. As outlined in the methods section, the number of PCs that we report on here is an arbitrary choice that was made because together they represent nearly 90% of total shape variation. Modern humans clearly separate from the archaic groups and overlap occurs between *H. heidelbergensis* s.l. and *H. neanderthalensis*, and slightly between *H. erectus* s.l. and *H. neanderthalensis*. Zuttiyeh, Jebel Irhoud 1, Dali and Bodo fall within the Neanderthal range, while Florisbad plots outside of all group ranges. Qafzeh 6, Skhul 5, and Zhoukoudian Upper Cave 101 plot adjacent to one another between archaic and modern humans and all Upper Paleolithic *H. sapiens* cluster with the recent modern humans except for Zhoukoudian Upper Cave 101 (see also Harvati, 2009). We tested the stability of the DFA results by including between five and 16 principal components of shape space. In all iterations, overlap variably occurred between Neanderthals, *H. heidelbergensis* s.l. and *H. erectus* s.l. Modern and Upper Paleolithic humans always clustered separately from the archaic hominins. The position of Zuttiyeh changed very little, always plotting with or near the Neanderthal sample.

Based on posterior probabilities, Zuttiyeh either classified as *H. heidelbergensis* s.l. or as a Neanderthal. Depending on how many principal components were used, the accuracy of correctly classifying fossils ranged from 55% to 73%. Shanidar 5 was most frequently classified as *H. erectus* s.l. and Arago 21 was always misclassified as *H. neanderthalensis* (it was originally assigned to *H. heidelbergensis* s.l.). Additionally, many fossils fluctuated between the three archaic groups (*H. erectus* s.l., *H. heidelbergensis* s.l. and *H. neanderthalensis*). The result of the permutation test (Table 3) indicated that the frontal and zygomatic morphology of *H. sapiens* was significantly different ($p < 0.002$) from all groups (*H. erectus* s.l., *H. heidelbergensis* s.l., and *H. neanderthalensis*) and that among the fossil groups only *H. neanderthalensis* and *H. erectus* s.l. was significantly different ($p < 0.013$) from one another.

Visualization – Procrustes superimposition

Zuttiyeh's nearest neighbor in terms of Procrustes distance is Shanidar 5. To illustrate the resemblances between these specimens, we superimposed the two individuals (Figure 8a–c). In Figure 8, Zuttiyeh is in white and Shanidar 5 is in semitransparent blue; therefore, the overlapping areas are represented by the

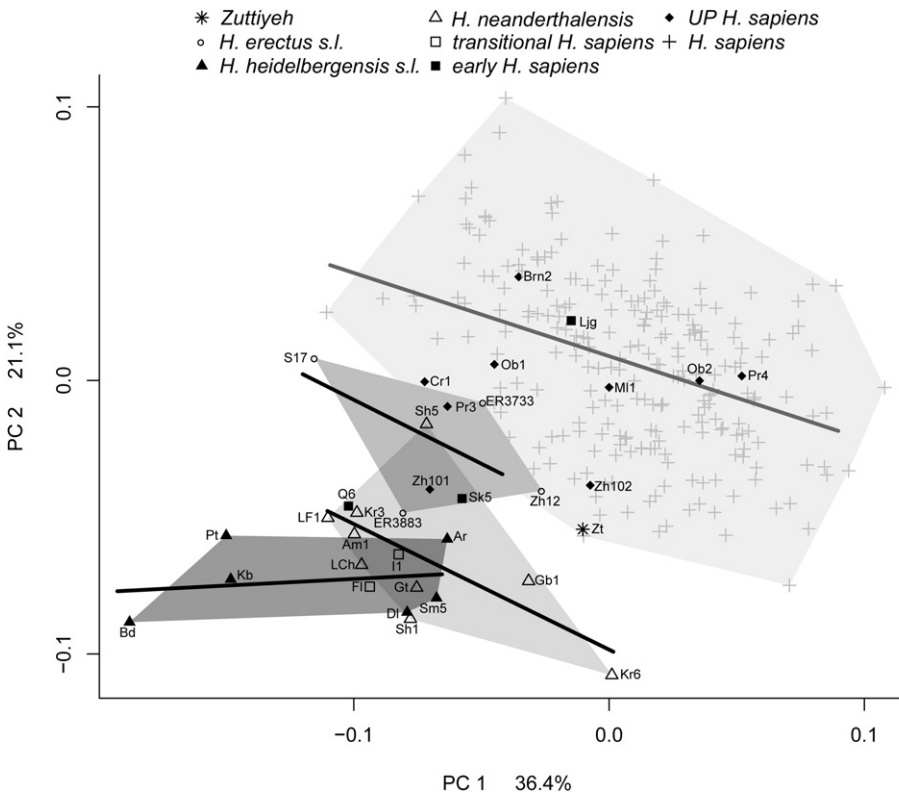

Figure 5. PCA in form space (including the centroid size of each specimen). PC 1 represents 36.4% of total form variation; PC 2 represents 21.1% of total form variation. Convex hulls are drawn for *H. erectus* s.l., *H. heidelbergensis* s.l., *H. neanderthalensis* and recent *H. sapiens* and the size trends, calculated by regressing shape on log centroid size, are represented by the black lines.

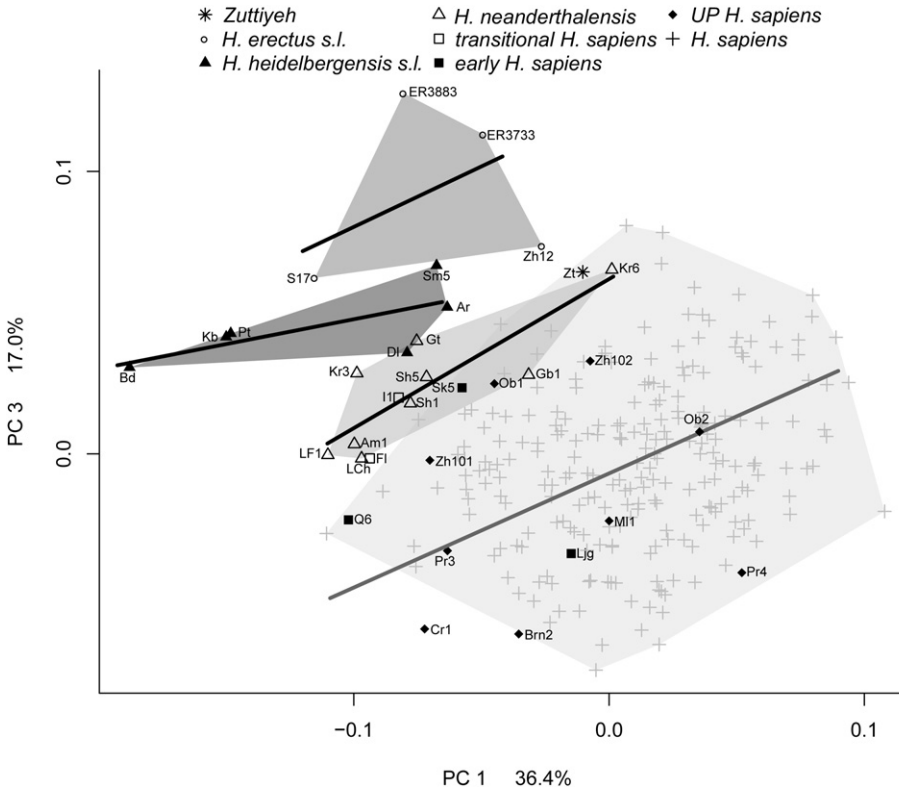

Figure 6. PCA in form space (including the centroid size of each specimen). PC 1 represents 36.4% of total form variation; PC 3 represents 17.0% of total form variation. Convex hulls are drawn for *H. erectus* s.l., *H. heidelbergensis* s.l., *H. neanderthalensis* and recent *H. sapiens* and the size trends, calculated by regressing shape on log centroid size, are represented by the black lines.

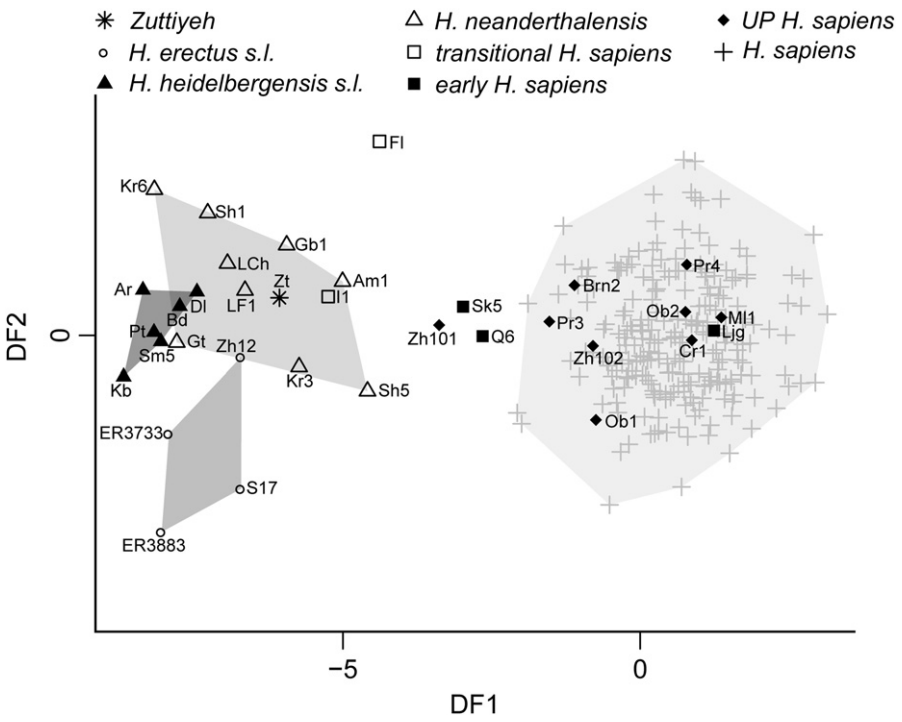

Figure 7. Discriminant function analysis using the first eight principal components of shape space, representing 87.3% of total shape variation. Convex hulls are drawn for *H. erectus* s.l., *H. heidelbergensis* s.l., *H. neanderthalensis* and recent *H. sapiens*. A priori groupings are listed in Table 1.

lighter shade of blue. Apart from the long anterior-posterior length of the frontal bone of Shanidar 5, these two specimens have similar frontal widths and frontal bone shapes. They both express a vertical frontal squama that then becomes more convex posteriorly. Shanidar 5 has a deeper medial post-toral sulcus and Zuttiyeh has a flatter glabellar region. Zuttiyeh's mid and upper face is entirely more robust than Shanidar 5 in the following ways: its nasal roots (i.e., area around nasion) project more anteriorly, it has a relatively greater inter-orbital breadth, it has an entirely larger and more projecting browridge, and the frontal process of the zygomatic bone and the posterior margin of the zygomatic body (i.e., fascia temporalis) are relatively wider. The angle at which the zygomatic bone (at the frontal process) meets the frontal bone and the rotation of the zygomatic body are similar between the two specimens.

Zuttiyeh's next nearest neighbor in shape space is Arago 21. In Figure 8d–f, we superimposed the two individuals. Arago 21 is in red and the overlapping areas are represented by the lighter shade of red. Zuttiyeh's frontal bone is more convex and its frontal squama is more vertical. The width of the frontal bone at frontotemporale is narrower in Zuttiyeh and its frontal bone becomes wider posteriorly. Zuttiyeh expresses a deeper post-toral sulcus region. The entire browridge and glabellar region of Arago 21 is slightly more projecting and is especially more robust at the lateral third. The orbital height is greater in Zuttiyeh, while the breadth and shape are similar between the two. Zuttiyeh has a wider inter-orbital breadth and its nasal root is more anteriorly projecting. The position of the zygomatic bone relative to the frontal bone is very similar. The frontal process of the zygomatic and the zygomatic body is larger and more robust in Arago 21 and the angle of the zygomatic at the medial margin (i.e., near the zygomaxillary suture) is more oblique indicative of its greater midfacial prognathism.

In Figure 9a–c, we warped Zuttiyeh to the *H. erectus* s.l. mean, in green, and superimposed the two. The frontal bone in Zuttiyeh is more convex and wider. Zuttiyeh has a deeper post-toral sulcus and a wider inter-orbital breadth. The orbital height, breadth and shape are similar between the two. The zygomatic bone in Zuttiyeh is much smaller in all dimensions compared with *H. erectus* s.l. The angle of the zygomatic body is remarkably similar between the two (see Figure 9c), however, in Zuttiyeh the angle of the zygomatic at the medial margin (i.e., near the zygomaxillary suture) is more oblique or anteriorly projecting. Overall, the mid and upper face is much more robust in *H. erectus* s.l., which exhibits a more projecting browridge, glabellar region, and nasal root and larger zygomatic bone.

In Figure 9d–f, we warped Zuttiyeh to the *H. heidelbergensis* s.l. mean, in red, and superimposed them. The frontal bone in Zuttiyeh is more convex and wider along the posterior half. The width at frontotemporale is narrower in Zuttiyeh. The overall browridge is much more robust and projecting in the *H. heidelbergensis* s.l. mean, especially in the medial third of the browridge and glabellar region. In both Zuttiyeh and the *H. heidelbergensis* s.l. mean, the nasal root is posterior to glabella, however, it appears more extreme in *H. heidelbergensis* because its glabellar region is much more projecting than Zuttiyeh. Zuttiyeh has a deeper post-toral sulcus. Its orbital height, breadth and shape are similar to the *H. heidelbergensis* s.l. mean, but the inter-orbital breadth is slightly larger in the *H. heidelbergensis* s.l. mean. The zygomatic bones are nearly the same size. The angle of the frontal process of the zygomatic, where

Table 3
Procrustes distances between mean configurations (upper) and significance values (lower). *P* values were computed using permutation tests on Procrustes distances from the mean. Significant values are denoted in bold.

	H. heidelbergensis s.l.	*H. erectus* s.l.	*H. neanderthalensis*	*H. sapiens*
H. heidelbergensis s.l.	–	0.0694	0.0487	0.1359
H. erectus s.l.	0.2167	–	0.0818	0.1306
H. neanderthalensis	0.3269	**$p < 0.0130$**	–	0.1025
H. sapiens	**$p < 0.0001$**	**$p < 0.0002$**	**$p < 0.0001$**	–

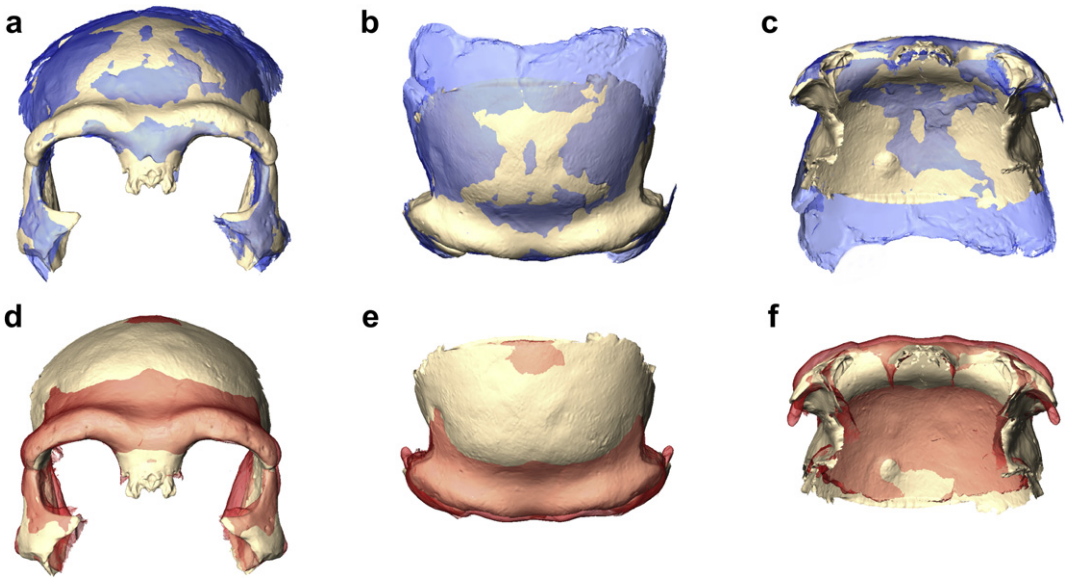

Figure 8. Procrustes superimpositions of Zuttiyeh on its nearest neighbors in shape space. Shape information is contained in the landmark and semilandmark data and everything in between these landmarks is interpolated. 8a–c (a – anterior perspective, b – superior, c – inferior): Zuttiyeh (white) superimposed on Shanidar 5 (blue), Zuttiyeh's nearest neighbor in shape space based on inter-individual Procrustes distances. 8d-f: Zuttiyeh (white) superimposed on Arago 21 (red), Zuttiyeh's second nearest neighbor in shape space based on inter-individual Procrustes distances. (For interpretation of the references to colour in this figure legend, the reader is referred to the web version of this article).

the zygomatic bone joins the frontal bone is very similar, but the frontal process of the *H. heidelbergensis* s.l. mean is much more robust and wider. The angle of the zygomatic body is different between the two: in the *H. heidelbergensis* s.l. mean the body is positioned posteriorly and is more sagitally rotated, and in Zuttiyeh the zygomatic body is positioned anteriorly and is more coronally rotated.

In Figure 9g–i, we warped Zuttiyeh to the Neanderthal mean, in blue, and superimposed them. Overall the frontal bone of Zuttiyeh is narrower and the posterior half is more convex. The width of the frontal bone at frontotemporale is nearly the same, but in the Neanderthal mean the frontal bone widens posterior to this region. The browridge shape is very similar between the two however in Zuttiyeh the lateral third of the browridge is much more robust. The Neanderthal glabellar region and nasal root is much more anteriorly projecting. In Zuttiyeh, the glabellar region is flattened and nasion and the nasal root are posterior to glabella. Like the comparison to *H. heidelbergensis* s.l., Zuttiyeh has a deeper posttoral sulcus, the orbital height, breadth and shape are similar between the two, but the inter-orbital breadth is slightly larger in the Neanderthal mean. The frontal process of the zygomatic is more robust in Zuttiyeh. In the Neanderthal mean, the zygomatic body is positioned posteriorly, rotated sagitally, and is flattened and retreating. In Zuttiyeh, the zygomatic body is positioned anteriorly and is rotated coronally. The Neanderthal zygomatic bones are smaller in all dimensions.

Lastly, in Figure 9j–l we warped Zuttiyeh to the modern human mean, in gray, and superimposed them. The modern human frontal bone is entirely more convex. They express a similar frontal bone width. The shape differences between the two are most pronounced in the mid and upper face. In Zuttiyeh, all aspects of its browridge size and shape and glabellar region are more robust than modern humans. Zuttiyeh's orbital height and breadth and interorbital breadth are larger. Although the zygomatic body in modern humans and in Zuttiyeh are similar in height (superoinferior dimension), the frontal process and posterior margin of the zygomatic body is much more robust in Zuttiyeh. This latter region is wider (e.g., more flaring) and more coronally rotated in Zuttiyeh than in the modern human mean, however, the angles of the medial margin of the zygomatic body where it approaches the zygomaxillary suture are similarly coronally rotated in both the modern human mean and Zuttiyeh.

Discussion

The aim of this study was to assess the morphological affinities of the Zuttiyeh fossil. Semilandmark geometric morphometric methods were employed to quantify the overall morphology of its frontal and zygomatic bone, multivariate statistics were performed to analyze the general pattern of morphological variation in Pleistocene fossils and modern humans, and visualization techniques were used to compare both the subtle and gross morphological differences among individual fossils and group means.

Nearest neighbors

Earlier studies have suggested that Zuttiyeh shows a resemblance to fossils such as Tabun 1 (McCown and Keith, 1939; Suzuki and Takai, 1970), Skhul 5 (Weidenreich, 1943), Ehringsdorf (Coon, 1963), Krapina (Coon, 1963), Zhoukoudian E1 (Hrdlička, 1930; Sohn and Wolpoff, 1993), Shanidar 1 (Suzuki and Takai, 1970), Shanidar 2 and 4 (Trinkaus, 1983) and Amud (Simmons et al., 1991). For various reasons (e.g., undiscovered fossils, different research questions, error in geological dates) most of these studies included a limited fossil sample, primarily consisting of Near Eastern hominins and European Neanderthals. Therefore Zuttiyeh's similarity to other Middle Pleistocene hominins has not been extensively explored.

Our results show that Zuttiyeh is morphologically most similar to Shanidar 5, a Near East Neanderthal, Arago 21, a European Middle Pleistocene hominin, and Skhul 5, an early *H. sapiens*. The main morphological similarities between Zuttiyeh and Shanidar 5 are the width of the frontal bone, the shape of the frontal squama and the angle of the zygomatic body. Following the original reconstruction of Shanidar 5, Trinkaus (1982, 1983) noted that the unusual combination of a flat frontal bone and curved parietal

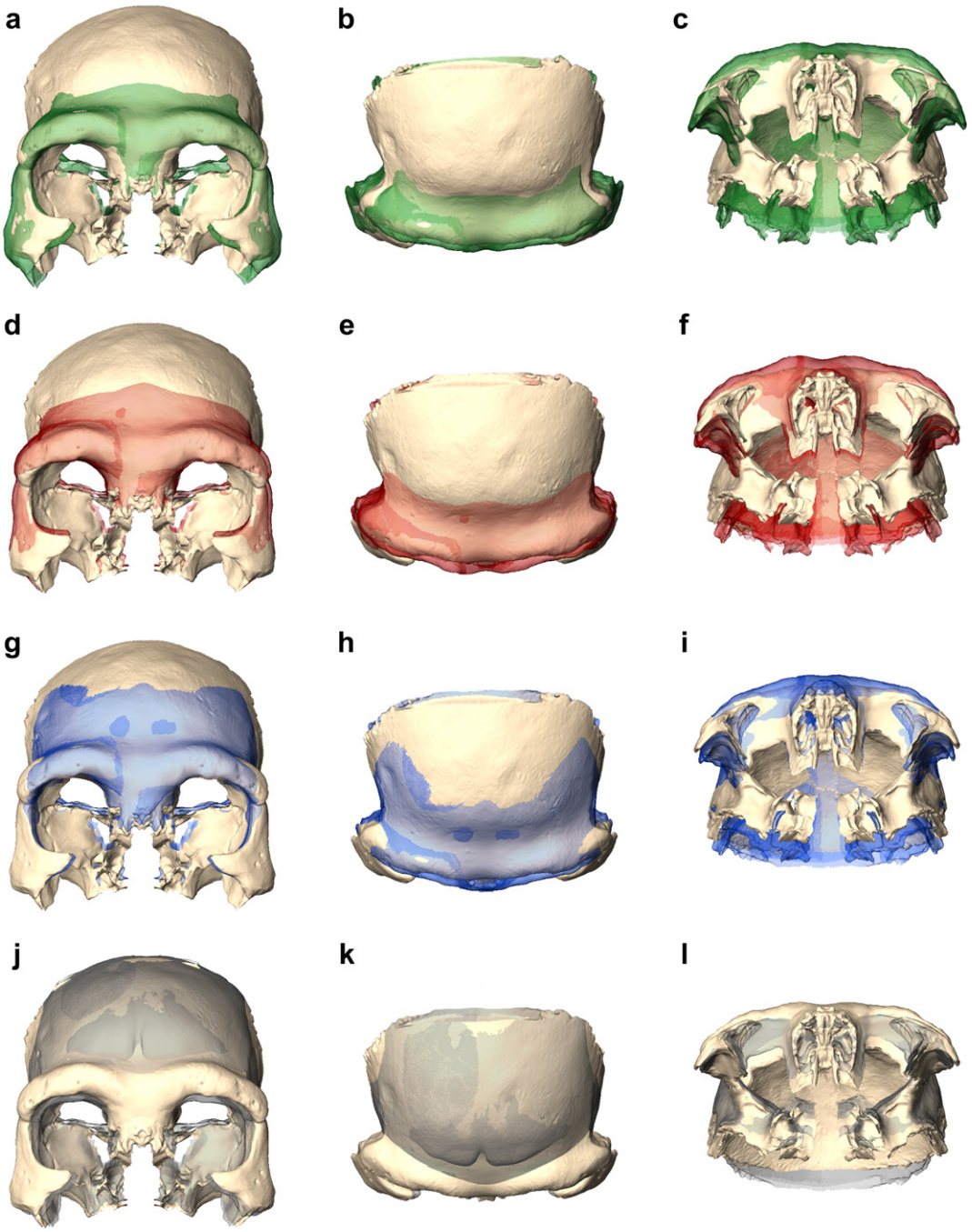

Figure 9. Procrustes superimpositions of Zuttiyeh on mean shapes. 9a–c (a – anterior perspective, b – superior, c – inferior): Zuttiyeh (white) superimposed on the *H. erectus* s.l. mean (green); 9d–f: superimposed on the *H. heidelbergensis* s.l. mean (red); 9g–i: superimposed on the *H. neanderthalensis* mean (blue); 9j–l: superimposed on the modern human mean (gray). (For interpretation of the references to colour in this figure legend, the reader is referred to the web version of this article).

bone, proportions similar only to Shanidar 1, may be due to artificial cranial deformation in these fossils. Because it was evident to Chech et al. (1999), that what was purported to be the left lambdoid suture was actually the left squamosal suture of the parietal bone, the Shanidar 5 cranium was reconstructed again in 1999. As a result, lambda is not present on the newest reconstruction of the Shanidar 5 cranium thereby eliminating the highly curved parietal arc (measured from bregma to lambda) previously perceived by Trinkaus (1982, 1983). A cast of the new reconstruction was used in this analysis. Apart from its extremely flat frontal bone, which is above the upper limit of the Neanderthal range, Shanidar 5 shows typical Neanderthal facial features (Trinkaus, 1983) and in our analyses (e.g., PCA and DFA) it falls within Neanderthal variation. As a result, we support the notion that its flattened frontal bone can be most likely attributed to individual or regional variation rather than artificial deformation (Chech et al., 1999). Unlike Simmons et al. (1991) and Athreya (2009), our analyses do not show any special affinities between Shanidar 1 and 5 to the exclusion of the other Near East Neanderthals (Tabun 1 and Amud 1). The discrepancy in our results may be due to our differing landmark and specimen data sets.

Among the Middle Pleistocene hominins, the European specimens Arago 21, Petralona and Sima de los Huesos 5, have been described as showing signs of incipient Neanderthal morphology in

their midface, including a flattened infraorbital surface topography and obliquely orientated zygomatics (Arsuaga et al., 1997; Dean et al., 1998; Hublin, 1998; but see; Harvati, 2009; Harvati et al., 2010). Our results show that the mid and upper face of Arago 21 is overall more robust compared with Zuttiyeh and that the main features shared between them are in the shape of the browridge and the angle of the zygomatic body. However, on Arago 21 the medial margin of the zygomatic at the zygomaxillary suture is angled more obliquely, indicative of greater midfacial prognathism. Therefore, the midface of Arago 21 is more similar to the Neanderthal condition than to Zuttiyeh.

It has been suggested that the distortion in Arago 21 may make it more gracile than it really is (Guipert, 2005; Guipert et al., 2007). In Guipert's (2005) reconstruction and subsequent analysis of Arago 21, he found it to be most similar to the Ceprano calvarium from Italy (Guipert, 2005; Guipert et al., 2007) that was recently re-dated to between 430 and 385 ka (Muttoni et al., 2009; Manzi et al., 2010). The Ceprano calvarium has been the focus of a several morphometric studies (Manzi et al., 2001; Bruner and Manzi, 2005; 2007) and like many of the other Middle Pleistocene neurocranial remains, its morphology is intermediate between *H. erectus* and *H. heidelbergensis/rhodesiensis* making its taxonomic affinities difficult to determine (Bruner and Manzi, 2005; 2007). Most recently, in a study that combined geometric morphometrics and scoring of discrete characters Mounier et al. (2011) suggested that Ceprano was an appropriate representative for the ancestral stock of a wide-ranging *H. heidelbergensis* (Mounier et al., 2011).

Subtle differences in morphology

Hrdlička (1930) and later Sohn and Wolpoff (1993) emphasized the morphological similarities between Zuttiyeh and the Lower Cave Zhoukoudian hominins. In their metrical analysis, Sohn and Wolpoff (1993) found that although Zuttiyeh was most similar to the Near Eastern Neanderthals, it also shared a unique frontal size, curvature, and dimensions of the lateral aspect of the supraorbital torus with the Zhoukoudian hominins. However, it must be noted that their comparative sample was limited to only the Near East Neanderthals, Skhul and Qafzeh, and the Lower Cave Zhoukoudian specimens. Additionally, in their qualitative comparisons Sohn and Wolpoff (1993) found striking similarities between Zuttiyeh and the Zhoukoudian, Gongwangling and Hexian (two Mid/Late Pleistocene hominins from China) *H. erectus* hominins. They claim that these hominins share a similar frontal shape, orbital shape, supraorbital configuration, flattened glabella and superior nasal region, and zygomatic orientation, which all contribute to a mid and upper facial flatness common in living Asian populations and their ancestors.

When we superimpose Zuttiyeh on the mean *H. erectus* s.l. shape, our results show clear differences in frontal bone shape. However, in the features related to mid and upper facial flatness listed by Sohn and Wolpoff (1993), they are quite similar. In both the PCA in shape space and the DFA, Zhoukoudian 12 plots near the Neanderthal range of variation, and in the DFA it is consistently misclassified as a Neanderthal. When PC 1 and 2 are plotted in Procrustes form space, Zuttiyeh plots near Zhoukoudian 12. These results suggest that Zhoukoudian 12 clearly shows some derived, possibly 'Neanderthal-like', zygomatic and/or frontal bone morphology, but its specific resemblances to Zuttiyeh may be primarily driven by size.

Vandermeersch (1989) argued that except for Zuttiyeh's strong browridge, its facial architecture is most similar to that of modern humans. He proposes that fewer morphological changes need to be made to go from Zuttiyeh to a modern human than from Zuttiyeh to a Neanderthal. These changes are reduction in browridge increase in frontal squama size, modification of the shape of the orbits from square to rectangular and low, and a reduction in overall robusticity. Features Vandermeersch (1989) cites as more modern human-like are an advanced degree of separation of the supraorbital torus into medial and lateral components, vertical frontal squama and high frontal elevation, and an anteriorly facing body of zygomatic.

Our superimposition results (Figure 9a–i) show that the anterior projection of the medial portion of the browridge is similar in all archaic groups and that the main differences between these groups are in the projection of the lateral browridge and glabellar region, which is greatest in *H. heidelbergensis* s.l. In Zuttiyeh, the height of the medial component of the torus is similar to *H. erectus* s.l. and Neanderthals, and the projection and height of the lateral component is smaller than in *H. heidelbergensis* s.l. and greater than *H. erectus* s.l. and Neanderthals. The glabellar region in Zuttiyeh, however, is much more gracile (i.e., less projecting) than in all of these groups. This is consistent with Athreya (2009), possibly supporting a female attribution for Zuttiyeh.

In their multivariate morphometric analysis of Southwest Asian frontal bones, Simmons et al. (1991) show the Zuttiyeh frontal bone to be more similar to Amud 1 than the Skhul/Qafzeh hominins. They argue that, because their results indicate that Zuttiyeh is more similar to a Neanderthal than an early modern human, their data fail to support the presence of a modern human-like high frontal bone and vertical frontal squama in Zuttiyeh. Our superimpositions (Figure 9j–l) show that the frontal bone elevation and shape in Zuttiyeh is more similar to modern humans than any of the archaic human mean shapes. However, Shanidar 5 (see Figure 8a–c) shares with Zuttiyeh a similar modern human-like vertical height in its frontal squama. The discrepancy between the results of Simmons et al. (1991) and our study is most likely due to methodological differences. Simmons et al. (1991) use traditional linear measurements (following Howells, 1973) to quantify the frontal bone shape. Geometric morphometrics and surface-semilandmarks, however, allow researchers to better capture more subtle morphological features, especially on smooth surfaces where osteometric landmarks are rare, like the frontal bone.

The final feature that Vandermeersch (1989) states as being modern human-like in Zuttiyeh is the anteriorly facing body of the zygomatic. Zuttiyeh's zygomatic body orientation is most like *H. erectus* s.l. mean shape (Figure 9c) and Shanidar 5 (Figure 8c), however the differences among the group mean shapes in this region are very subtle. Although Zuttiyeh is missing both maxillae, the orientation of its zygomatic bones, especially along the zygomaxillary suture, can provide an indication of its overall facial prognathism. When the superimpositions are viewed from an inferior perspective (Figure 9c, f, i and l) and compared between the archaic and modern human means, one can see that the zygomaxillary border of the zygomatic in Zuttiyeh is more anteriorly projecting than in the *H. erectus* s.l. mean, suggesting a slightly greater midfacial prognathism in the former. Regarding this feature, our results support Simmons et al. (1991) who propose that Zuttiyeh has a total facial prognathism combined with a flat zygomatic, like that of African *H. erectus*, Petralona, Broken Hill and Shanidar 4.

Shanidar 4 along with Shanidar 2, 6, 7, 8 and 9 were found in an archaeological layer lower than Shanidar 1 and 5. The faces of Shanidar 2 and 4 have been described as expressing greater robusticity and less midfacial prognathism than the later Shanidar Neanderthals 1 and 5 and European Neanderthals (Trinkaus, 1983). According to Trinkaus (1983), these features align them more with the earlier Near East (Zuttiyeh) and European specimens (Petralona, Arago 21, Steinheim). Unfortunately, we were not able to include these specimens in our analysis.

General morphological patterns

The first two dimensions of the PCA in shape space of the frontal and zygomatic bones are dominated by the contrast between fossil and modern humans (including the Upper Paleolithic specimens), with overlap primarily occurring between the Middle to Late Pleistocene groups (*H. heidelbergensis* s.l., *H. neanderthalensis*, transitional *H. sapiens* and early *H. sapiens*) and Zhoukoudian Upper Cave 101 and 102. The dichotomy in craniofacial morphology between archaic and recent humans has been recognized in past studies (e.g., Howells, 1970; Stringer, 1974) as well as several recent morphometric analyses (Weber et al., 2006; Harvati, 2009; Athreya, 2009; Gunz et al., 2009a; Stansfield and Gunz, 2011). In Athreya's (2009) quantitative study of frontal bone morphology in Pleistocene fossil hominins, she found that in most aspects archaic human populations (*H. erectus* s.l., *H. heidelbergensis* s.l., *H. neanderthalensis*) are not significantly different from each other, and that anatomically modern humans (early, Upper Paleolithic, and recent *H. sapiens*) have the most distinctive frontal bones. Similarly, in geometric morphometric analyses of Pleistocene hominin neurocrania and faces, Weber et al. (2006), Gunz et al. (2009a) and Harvati et al. (2007; see also Harvati, 2009) show that the greatest shape differences to be between archaic and anatomically modern humans (fossil and recent). In each of these geometric morphometric analyses, the tightest clustering appears to be between the Neanderthals and non-habiline archaic *Homo* (i.e., *H. erectus* s.l. and *H. heidelbergensis* s.l.). Several authors have suggested that Neanderthals and archaic *Homo* share a conserved neurocranial architecture that is different from modern humans (Lieberman et al., 2002; Bruner et al., 2003; Trinkaus, 2007; Gunz et al., 2009a). Our results also confirm this observation in the frontal bone.

As illustrated in Figure 3a–d, the main morphological shape changes along PC 1 are in the width and shape of the frontal bone, projection of the browridge and overall size and robusticity of the mid and upper face. Plotting on the negative end of PC 1, the *H. erectus* s.l. and *H. heidelbergensis* s.l. specimens express one extreme version of this morphology exhibiting a narrower and more receding (i.e., flatter) frontal bone in combination with a wider, more projecting and entirely more robust browridge and larger zygomatic bones in all dimensions. Among the Middle Pleistocene specimens, this morphology is most apparent in Bodo, Kabwe and Petralona. Massive supraorbital tori and flattened frontals are two ubiquitous features in *H. erectus* that have been suggested to have been retained in Middle Pleistocene hominins (Rightmire, 2007). Our PCA results in Procrustes shape and form space suggest that this might be true for Bodo, Kabwe and Petralona. Athreya (2009), van Vark (1995) and Rightmire (2001) also found these specimens to be the most morphologically similar to each other, indicating that they are all male and/or part of the same taxonomic group.

As in the PCA, the results of the DFA show that *H. heidelbergensis* s.l. and *H. neanderthalensis* share a very similar fronto-zygomatic morphology; Dali, Bodo, and Zuttiyeh cluster within the range of Neanderthal variation. The lack of stability in the DFA and classification analysis is caused by the similarities in frontal and zygomatic morphology between these two archaic groups. This is further corroborated by the permutation test, which shows that apart from Neanderthals and *H. erectus* s.l., there are no significant differences in frontal and zygomatic bone shape between the fossil human groups. The similarities between the *H. heidelbergensis* s.l. and Neanderthal morphology are especially apparent in the Procrustes superimposition figures of Zuttiyeh and the Neanderthal mean (Figure 9g–i) and Zuttiyeh and the *H. heidelbergensis* mean (Figure 9d–f). These two groups share an archaic browridge and frontal bone morphology. A great level of similarity between African and European *H. heidelbergensis* s.l. specimens, as well as between them and Neanderthals, in facial morphology was found in previous, landmark-based studies of facial variability (Harvati, 2009; Harvati et al., 2010), and is confirmed here, although, unlike this previous work, the present study involves only a subset of the face.

Taken together, a comparison of mean shapes shows that subtle differences can be identified in frontal and zygomatic bone morphology among *H. erectus* s.l., *H. heidelbergensis* s.l., and *H. neanderthalensis*. However, these shape differences are minor variations on a common theme and not great enough to statistically discriminate distinct morphological groups among the Middle to Late Pleistocene hominins. Our results are congruent with Athreya (2009) and show that the frontal bone morphology is not sufficient for differentiating the Middle to Late Pleistocene human fossil groups.

Evolutionary implications

There are four evolutionary scenarios that might explain the morphology of the Zuttiyeh specimen in the context of the Southwest Asian fossil record. First, Zuttiyeh was a local member of a geographically wide-ranging Middle Pleistocene species that was also present in Africa and Europe. According to our results, both Zuttiyeh's phenetic similarities to Arago 21 and the clustering of the African and European Middle Pleistocene hominins in our PCA and DFA supports this scenario. This scenario is in accordance with the late divergence model of modern human origins, which emphasizes the strong similarities in the human fossil record between Africa, Europe and possibly Asia (Hublin, 2009). Supporters of this model see the Middle Pleistocene hominins across these continents as representing one species, possibly *H. heidelbergensis* (or *Homo rhodesiensis* if the Mauer mandible is not included in this group; see Hublin, 2009), the last common ancestor of Neanderthals and modern humans (Rightmire, 1998b; Stringer, 2002; Mounier et al., 2009; 2011).

Second, according to the accretionary model of Neanderthal evolution (see Dean et al., 1998; Hublin, 1998; 2009), there was a long term in situ evolution of Neanderthals in Western Eurasia and Zuttiyeh was a southwestern member of this group designated as *H. neanderthalensis* (Hublin, 2009) or as *H. heidelbergensis* s.s. (Arsuaga et al., 1997); a chronospecies directly ancestral to Neanderthals. Phenetic similarities shared between Zuttiyeh and Shanidar 5 may support this scenario.

Third, there was regular gene flow between Africa and Western Asia during the Middle to Late Pleistocene and Zuttiyeh was a member of the population ancestral to *H. sapiens* in Africa. Following Woodward (1921), *H. rhodesiensis* has been proposed as the name of the taxon for the African group. Our results do not support any direct link between Zuttiyeh and the African Middle Pleistocene humans to the exclusion of the contemporaneous European populations, or to *H. sapiens*. However, the new Middle Pleistocene dental remains from the site of Qesem Cave in Israel, dated to between 400 and 200 ka, equivocally suggest a closer similarity to the Skhul and Qafzeh material than to Neanderthals (Hershkovitz et al., 2011). In addition to being from the same region and possibly the same time period, Zuttiyeh and the Qesem material also shared the Acheulo-Yabrudian lithic technology. Therefore, they may be part of the same local Middle Pleistocene *Homo* population, however, because they lack similarly preserved morphology we cannot directly compare them. Nevertheless, if they were members of the same population, then they were characterized by a mosaic pattern of craniodental morphology.

Fourth, Zuttiyeh and the Southwest Asian hominins (e.g., Skhul, Qafzeh and the Neanderthals) represent either a regional lineage of *H. sapiens* (Wolpoff et al., 1984), or, together with the African Mid-Late Pleistocene humans, they constitute a 'deep-rooted' *H. sapiens* lineage (Arensburg and Belfer-Cohen, 1998). According to this scenario, Zuttiyeh should show its closest affinities to the Southwest Asian hominins.

Our results can support any one of these models. According to our Procrustes distance calculations, the diversity of fossil types (e.g., African and European Middle Pleistocene humans, Near East Neanderthal and modern humans, Asian *H. erectus*, recent modern human) to which Zuttiyeh is most morphologically similar to (Figure 4) strongly suggest that it exhibits a generalized morphology, which one would expect to see in the last common ancestor of Neanderthals and modern humans. Therefore, while our results do not show strong support for one particular taxonomic allocation for the Zuttiyeh fossil, we advocate that its mosaic morphological pattern is indicative of the population that gave rise to Neanderthals and modern humans.

Neanderthals retained aspects of this ancestral frontal bone morphology and through time developed apomorphies on other parts of the cranium (e.g., suprainiac fossa, inflated maxillary region) that are characteristic of the classic European Neanderthals dated to Oxygen Isotope Stages 3 and 4 (Dean et al., 1998; Hublin, 1998; 2009). The evolutionary processes responsible (i.e., natural selection or genetic drift) for producing cranial differences between modern humans and Neanderthals are difficult to prove (see Lieberman, 2008). However, recent quantitative genetic and morphological studies suggest that genetic drift (neutral evolution) may have played an important role (Weaver et al., 2007; Roseman and Weaver, 2007; von Cramon-Taubadel and Lycett, 2008; Schillaci, 2008), although selection has also been suggested, especially for some aspects of the face (Weaver et al., 2007; Hubbe et al., 2009). Further evidence for the role of genetic drift in shaping the Neanderthal cranium is the gradual accumulation of Neanderthal features in the fossil record for over a period of >300,00 years (Hublin, 1998; 2009; Weaver, 2009).

This study is limited to the available anatomical information preserved on the Zuttiyeh fossil, namely the frontal and zygomatic morphology. Although the efficacy of using craniodental morphology to reconstruct phylogenetic hypothesis about human evolution has been questioned (see Collard and Wood, 2000), multiple recent studies on modern humans have found that overall cranial morphology reflects population history (e.g., Relethford, 1994; 2004a,b; Roseman, 2004; Harvati and Weaver, 2006a,b; Smith, 2009; Hubbe et al., 2009; von Cramon-Taubadel, 2009). However, the phylogenetic value of different anatomical regions (such as the face, vault or basicranium) remains open to debate. With reference to the specific anatomy preserved on Zuttiyeh, the cranial vault has been reported to be relatively highly correlated with population history (e.g., neutral genetic data or geographic distances; Roseman, 2004; Harvati and Weaver, 2006a,b; Hubbe et al., 2009), while the phylogenetic usefulness of facial morphology has been questioned, being potentially affected by climatic variables and/or mastication (e.g., Skelton and McHenry, 1992; Wood and Lieberman, 2001; Lieberman et al., 2004; Lieberman, 2008). Recent work testing this hypothesis has produced somewhat contradictory results (see Harvati and Weaver, 2006b; Hubbe et al., 2009; Smith, 2009). A study by von Cramon-Taubadel (2009) examined individual cranial bones as well as cranial regions among geographically diverse modern human populations and found that the maxilla, the zygomatic and the occipital bone are less reliable for reconstructing phylogenetic relationships. However, the majority of these studies were conducted on the microevolutionary scale and therefore may not be relevant for higher-level systematics.

Conclusion

This is the most detailed metrical study on the fronto-zygomatic region of Zuttiyeh to date. In the PCA and DFA, Zuttiyeh plots in the middle of the Neanderthal variation, and according to Procrustes distances it is phenetically most similar to Shanidar 5. In addition to sharing some similarities in zygomatic bone morphology, Shanidar 5 and Zuttiyeh also express a vertical frontal squama, a feature that is most often attributed to modern humans. However, in all other aspects its mid and upper facial morphology expresses a combination of features seen in Early to Late Pleistocene archaic humans. Overall, it is morphologically most similar to a Near East Neanderthal (Shanidar 5), a Middle Pleistocene hominin (Arago 21), and a Near East early modern human (Skhul 5).

This raises the intriguing possibility that the generalized morphology present in Zuttiyeh characterizes a population ancestral to both Neanderthals and modern humans, or a population immediately postdating their divergence. Hopefully, future fossil discoveries from this time period and geographical region, like in Qesem Cave in Israel, will shed more light on this issue. We conclude that Neanderthals largely retained a generalized morphology, while the modern human frontal and zygomatic bone represents a significant departure from this presumably ancestral morphology. Furthermore, these results show that the frontal and zygomatic bones are not sufficient for distinguishing archaic humans and that additional anatomical features should be used to allocate fossils.

Through the application of semilandmark geometric morphometric methods, we are able to provide quantitative support for the subtle differences in frontal and zygomatic bone morphology often described, or qualitatively identified, between the different archaic human groups used in this study (*H. erectus* s.l., *H. heidelbergensis* s.l., and *H. neanderthalensis).* However, the morphological differences among these groups are ultimately minor variations on a common theme and do not reflect underlying architectural differences. There is significant overlap between *H. heidelbergensis* s.l., Neanderthals and even early *H. sapiens*, indicating that all of these groups resemble the ancestral morphology. Only recent and most Upper Paleolithic modern humans depart from this pattern.

Acknowledgements

We would like to thank all of the curators who have so generously allowed us to scan the fossil and modern human material from the following institutions: American Museum of Natural History (New York), Aristotle University of Thessaloniki, Hrvatski Prirodoslovni Muzej (Zagreb), Institut de Paléontologie Humaine (Paris), Musée Archéologique (Rabat), Musée de l'Homme (Paris), Museo Nazionale Preistorico Etnografico 'L. Pigorini' (Rome), National Museum of Ethiopia (Addis Ababa), Natural History Museum (London), Naturhistorisches Museum (Vienna), Peabody Museum at Harvard University (Cambridge), Rheinisches Landesmuseum (Bonn), South African Museum (Cape Town), and the University of Cape Town. The authors show their deepest gratitude to Dr. David Begun, the Associate Editor and the two anonymous reviewers whose comments have improved the quality of the paper. We would also like to thank Dr. Yoel Rak, Ibrahim Fawzi and Alon Barah for their generous assistance in Israel, Dr. Fred Grine for allowing us to use some CT scans in our modern human comparative sample, and Dr. Eric Delson for his comments on earlier drafts of this manuscript. This work was supported by the Marie Curie Actions grant MRTN-CT-2005-019564 'EVAN,' the Max Planck Society, NSF (0333415, 0513660 and 0851756), the L.S.B. Leakey Foundation, and the Sigma Xi Foundation. This is NYCEP Morphometrics contribution 43.

Appendix. Supplementary material

Supplementary material associated with this article can be found, in the online version, at doi:10.1016/j.jhevol.2011.11.005.

References

Antón, S.C., 2002. Evolutionary significance of cranial variation in Asian *Homo erectus*. Am. J. Phys. Anthropol. 118, 301–323.

Antón, S.C., 2003. Natural history of *Homo erectus*. Am. J. Phys. Anthropol. S37, 126–170.

Antón, S.C., Swisher III, C.C., 2004. Early dispersals of *Homo* from Africa. Ann. Rev. Anthropol. 33, 271–296.

Arensburg, B., Belfer-Cohen, A., 1998. Sapiens and Neandertals: rethinking the Levantine Middle Paleolithic hominids. In: Akazawa, T., Aoki, K., Bar-Yosef, O. (Eds.), Neandertals and Modern Humans in Western Asia. Plenum Press, New York, pp. 311–322.

Arsuaga, J.L., Martínez, I., Gracia, A., Lorenzo, C., 1997. The Sima de los Huesos crania (Sierra de Atapuerca, Spain). A comparative study. J. Hum. Evol. 33, 219–281.

Asfaw, B., Gilbert, W.H., Beyene, Y., Hart, W.K., Renne, P.R., Wolde Gabriel, G., Vrba, E.S., White, T.D., 2002. Remains of *Homo erectus* from Bouri, Middle Awash, Ethiopia. Nature 416, 317–320.

Athreya, S., 2009. A comparative study of frontal bone morphology among Pleistocene hominin fossil groups. J. Hum. Evol. 57, 786–804.

Baab, K.L., 2008. The taxonomic implications of cranial shape variation in *Homo erectus*. J. Hum. Evol. 54, 827–847.

Bar-Yosef, O., 1988. The date of South-West Asian Neandertals. In: Otte, M. (Ed.), L'Homme de Neandertal. Etudes et Recherches Archéologiques de l'Université de Liège, Liège, pp. 31–38.

Bar-Yosef, O., 1989. Geochronology of the Levantine Middle Paleolithic. In: Mellars, P., Stringer, C. (Eds.), The Human Revolution. Edinburgh University Press, Edinburgh, pp. 589–610.

Bar-Yosef, O., 1992. The role of Western Asia in modern human origins. Phil. Trans. R. Soc. 337, 193–200.

Bischoff, J.L., Williams, R.W., Rosenbauer, R.J., Aramburu, A., Arsuaga, J.L., Garcia, N., Cuenca-Bescos, G., 2007. High-resolution U-series dates from the Sima de los Huesos hominids yields 600± kyrs: implications for the evolution of the early Neanderthal lineage. J. Archaeol. Sci. 34, 763–770.

Bookstein, F.L., 1991. Morphometric Tools for Landmark Data: Geometry and Biology. Cambridge University Press, Cambridge.

Bookstein, F.L., 1997. Landmark methods for forms without landmarks: morphometrics of group differences in outline shape. Med. Image. Anals 1, 225–243.

Bookstein, F.L., 2005. After landmarks. In: Slice, D.E. (Ed.), Modern Morphometrics in Physical Anthropology. Kluwer Academic/Plenum Publishers, New York, pp. 49–71.

Brown, P., 1992. Recent human evolution in East Asia and Australasia. Philos. Trans. R. Soc. Lond. 337, 235–242.

Bruner, E., Manzi, G., 2005. CT-based description and phyletic evaluation of the archaic human calvarium from Ceprano, Italy. Anat. Rec. A 285, 643–658.

Bruner, E., Manzi, G., 2007. Landmark-based shape analysis of the archaic *Homo* calvarium from Ceprano (Italy). Am. J. Phys. Anthropol. 132, 355–366.

Bruner, E., Manzi, G., Arsuaga, J.L., 2003. Encephalization and allometric trajectories in the genus *Homo*: evidence from the Neandertal and modern lineages. Proc. Natl. Acad. Sci. 100, 15335–15340.

Chech, M., Groves, A., Thorne, A., Trinkaus, E., 1999. A new reconstruction of the Shanidar 5 cranium. Paléorient 25, 143–146.

Chen, T., Hedges, R.E.M., Yuan, Z., 1989. Accelerator radiocarbon dating for the Upper Cave of Zhoukoudian. Acta Anthropol. Sinica 8, 216–221.

Chen, T., Zhang, Y., 1991. Paleolithic chronology and possible coexistence of *Homo erectus* and *Homo sapiens* in China. World Archaeol. 23, 147–154.

Clark, J.D., De Heinzelin, J., Schick, K.D., Hart, W.K., White, T.D., Wolde Gabriel, G., Walter, R.C., Suwa, G., Asfaw, B., Vrba, E., 1994. African *Homo erectus*: old radiometric ages and young Oldowan assemblages in the Middle Awash Valley, Ethiopia. Science 264, 1907.

Collard, M., Wood, B., 2000. How reliable are human phylogenetic hypotheses? Proc. Natl. Acad. Sci. 97, 5003–5006.

Cook, J., Stringer, C.B., Currant, A.P., Schwarcz, H.P., Wintle, A.G., 1982. A review of the chronology of the European Middle Pleistocene hominid record. Am. J. Phys. Anthropol. 25, 19–65.

Coon, C.S., 1963. Origin of Races. Knopf, New York.

de Lumley, H., de Lumley, M., 1971. Découverte de restes humaines anténéandertaliens datés au début de Riss à la Caune d'Arago (Tautavel, Pyrénées-Orientales). C. R. Acad. Sci. 272, 1729–1742. Paris.

Dean, D., Hublin, J.J., Holloway, R., Ziegler, R., 1998. On the phylogenetic position of the pre-neandertal specimen from Reilingen, Germany. J. Hum. Evol. 34, 485–508.

Dryden, I.L., Mardia, K.V., 1998. Statistical Shape Analysis. John Wiley & Sons, Chichester.

Falguères, C., Yokoyama, Y., Shen, G., Bischoff, J.L., Ku, T.L., de Lumley, H., 2004. New U-series dates at the Caune de l'Arago, France. J. Archaeol. Sci. 31, 941–952.

Feibel, C.S., Brown, F.H., McDougall, I., 1989. Stratigraphic context of fossil hominids from the Omo group deposits: northern Turkana Basin, Kenya and Ethiopia. Am. J. Phys. Anthropol. 78, 595–622.

Frayer, D.W., Wolpoff, M.H., Thorne, A.G., Smith, F.H., Pope, G.G., 1993. Theories of modern human origins: the paleontological test. Am. Anthropol. 95, 14–50.

Freidline, S.E., Gunz, P., Harvati, K., Delson, E., Hublin, J.J., 2008. How three-dimensional surface data can be used to reconstruct fragmentary fossils. Am. J. Phys. Anthropol. S46, 99.

Freidline, S.E., Gunz, P., Harvati, K., Hublin, J., 2010. 3D semilandmark geometric morphometric quantification of modern human facial development. Am. J. Phys. Anthropol. S50, 93.

Gisis, I., Bar-Yosef, O., 1974. New excavations in Zuttiyeh Cave. Paléorient 2, 175–180.

Glantz, M., Athreya, S., Ritzman, T., 2009. Is Central Asia the eastern outpost of the Neandertal range? A reassessment of the Teshik-Tash child. Am. J. Phys. Anthropol. 138, 45–61.

Green, R.E., Krause, J., Briggs, A.W., Maricic, T., Stenzel, U., Kircher, M., Patterson, N., Li, H., Zhai, W., et al., 2010. A draft sequence of the Neandertal genome. Science 328, 710–722.

Grine, F.E., Gunz, P., Betti-Nash, L., Neubauer, S., Morris, A.G., 2010. Reconstruction of the Late Pleistocene human skull from Hofmeyr, South Africa. J. Hum. Evol. 59, 1–15.

Grün, G.R., 1996. A re-analysis of electron spin resonance dating results associated with the Petralona hominid. J. Hum. Evol. 30, 227–241.

Grün, G.R., Huang, P.-H., Wu, X., Stringer, C.B., Thorne, A.G., McCulloch, M., 1997. ESR analysis of teeth from the palaeoanthropological site of Zhoukoudian, China. J. Hum. Evol. 32, 83–91.

Grün, G.R., Stringer, C.B., 1991. ESR dating and the evolution of modern humans. Archaeometry 33, 153–199.

Grün, G.R., Stringer, C.B., McDermott, F., Nathan, R., Porat, N., Robertson, S., Taylor, L., Mortimer, G., Eggins, S., McCulloch, M., 2005. U-series and ESR analyses of bones and teeth relating to the human burials from Skhul. J. Hum. Evol. 49, 316–334.

Guipert, G., 2005. Reconstitution et position phylétique des restes crâniens de l'homme de Tautavel (Arago 21-47) et de Biache-Saint-Vaast 2 apports de l'imagerie et de l'analyse tridimensionelles. Ph.D. Dissertation, Université Paul Cézane.

Guipert, G., Mafart, B., de Lumley, M.-A., 2007. Virtual Restoration of the Fossil Arago 21–47 and Phyletic Position (Abstract). Paleoanthropology Society, Philadelphia, PA.

Gunz, P., Mitteroecker, P., Bookstein, F., 2005. Semilandmarks in three dimensions. In: Slice, D.E. (Ed.), Modern Morphometrics in Physical Anthropology. Plenum Publishers, New York, pp. 73–98.

Gunz, P., Bookstein, F.L., Mitteroecker, P., Stadlmayr, A., Seidler, H., Weber, G.W., 2009a. Early modern human diversity suggests subdivided population structure and a complex out-of-Africa scenario. Proc. Natl. Acad. Sci. 106, 6094–6098.

Gunz, P., Harvati, K., 2007. The Neanderthal "chignon": variation, integration, and homology. J. Hum. Evol. 52, 262–274.

Gunz, P., 2005. Statistical and geometric reconstruction of hominid crania: reconstructing australopithecine ontogeny. Ph.D. Dissertation, University of Vienna.

Gunz, P., Mitteroecker, P., Neubauer, S., Weber, G.W., Bookstein, F.L., 2009b. Principles for the virtual reconstruction of hominin crania. J. Hum. Evol. 57, 48–62.

Gunz, P., Neubauer, S., Maureille, B., Hublin, J.J., 2010. Brain development after birth differs between Neanderthals and modern humans. Curr. Biol. 20, R921–R922.

Harvati, K., 2003a. The Neanderthal taxonomic position: models of intra- and interspecific craniofacial variation. J. Hum. Evol. 44, 107–132.

Harvati, K., 2003b. Quantitative analysis of Neanderthal temporal bone morphology using three-dimensional geometric morphometrics. Am. J. Phys. Anthropol. 120, 323–338.

Harvati, K., 2009. Into Eurasia: a geometric morphometric re-assessment of the Upper Cave (Zhoukoudian) specimens. J. Hum. Evol. 57, 751–762.

Harvati, K., Gunz, P., Grigorescu, D., 2007. Cioclovina (Romania): affinities of an early modern European. J. Hum. Evol. 53, 732–746.

Harvati, K., Hublin, J.J., Gunz, P., 2010. Evolution of Middle-Late Pleistocene human cranio-facial form: a 3-D approach. J. Hum. Evol. 59, 445–464.

Harvati, K., Panagopoulou, E., Runnels, C., 2009. The paleoanthropology of Greece. Evol. Anthropol. 18, 131–143.

Harvati, K., Weaver, T.D., 2006a. Human cranial anatomy and the differential preservation of population history and climate signatures. Anat. Rec. A. 288, 1225–1233.

Harvati, K., Weaver, T.D., 2006b. Reliability of Cranial Morphology in Reconstructing Neanderthal Phylogeny. Neanderthals Revisited: New Approaches and Perspectives. Springer, Dordrecht, pp. 239–254.

Hedges, R.E.M., Housley, R.A., Bronk, C.R., Van Klinken, G.J., 1992. Radiocarbon dates from the Oxford AMS system: archaeometry Datelist 14. Archaeometry 34, 141–159.

Hershkovitz, I., Smith, P., Sarig, R., Quam, R., Rodríguez, L., García, R., Arsuaga, J.L., Barkai, R., Gopher, A., 2011. Middle Pleistocene dental remains from Qesem Cave (Israel). Am. J. Phys. Anthropol. 144, 575–592.

Hodgson, J.A., Bergey, C.M., Disotell, T.R., 2010. Neandertal genome: the ins and outs of African genetic diversity. Curr. Biol. 20, R517–R519.

Holt, B.M., Formicola, V., 2008. Hunters of the Ice Age: the biology of Upper Paleolithic people. Am. J. Phys. Anthropol. S47, 70–99.

Howells, W.W., 1970. Mount Carmel man: morphological relationships. In: Proceedings, 8th International Congress of Anthropological and Ethnological Sciences, 1, pp. 269–272.

Howells, W.W., 1973. Cranial Variation in Man: A Study by Multivariate Analysis of Patterns of Differences Among Recent Human Populations (Papers of the Peabody Museum of Archaeology and Ethnology, Harvard, Cambridge).

Hrdlička, A., 1930. The Skeletal Remains of Early Man. Smithsonian Institution Annual Report for 1928. The Smithsonian Institution, Washington D.C, pp. 593–623.
Hubbe, M., Hanihara, T., Harvati, K., 2009. Climate signatures in the morphological differentiation of worldwide modern human populations. Anat. Rec. 292, 1720–1733.
Hublin, J.-J., 1998. Climate changes, paleogeography, and the evolution of the Neandertals. In: Akazawa, T., Bar-Yosef, O. (Eds.), Neandertals and Modern Humans in Western Asia. Plenum Press, New York, pp. 295–310.
Hublin, J.-J., 2009. Out of Africa: modern human origins special feature: the origin of Neandertals. Proc. Natl. Acad. Sci. 106, 16022–16027.
Huxtable, J., 1990. Burnt Flint Date for Yabrud Shelter I Ancient TL Date Lists No. 4 Entry 43.
Keith, A., 1927. A report on the Galilee skull. In: Turville-Pétre, F. (Ed.), Researches in Prehistoric Galilee, 1925–1926. Council of the British School of Archaeology in Jerusalem, London, pp. 593–623.
Klein, R.G., 1994. Southern Africa before the Iron age. In: Corruccini, R.S. (Ed.), Integrative Paths to the Past: Paleoanthropological Advances in Honor of F. Clark Howell. Prentice Hall, Engelwood Cliffs, N.J, pp. 471–519.
Klein, R.G., 1999. The Human Career. The University of Chicago Press, Chicago.
Larick, R., Ciochon, R.L., Zaim, Y., Sudijono, Suminto, Rizal, Y., Aziz, F., Reagan, M., Heizler, M., 2001. Early Pleistocene $^{40}Ar/^{39}Ar$ ages for Bapang Formation hominins, Central Java, Indonesia. Proc. Natl. Acad. Sci. 98, 4866–4871.
Lieberman, D.E., 2008. Speculations about the selective basis for modern human craniofacial form. Evol. Anthropol. 17, 55.
Lieberman, D.E., McBratney, B.M., Krovitz, G., 2002. The evolution and development of cranial form in *Homo sapiens*. Proc. Natl. Acad. Sci. 99, 1134–1139.
Lieberman, D.E., Krovitz, G.E., Yates, F.W., Devlin, M., St Claire, M., 2004. Effects of food processing on masticatory strain and craniofacial growth in a retrognathic face. J. Hum. Evol. 46, 655–677.
Manzi, G., Magri, D., Milli, S., Palombo, M.R., Margari, V., Celiberti, V., Barbieri, M., Barbieri, M., Melis, R.T., et al., 2010. The new chronology of the Ceprano calvarium (Italy). J. Hum. Evol. 59, 580–585.
Manzi, G., Mallegni, F., Ascenzi, A., 2001. A cranium for the earliest Europeans: phylogenetic position of the hominid from Ceprano. Italy. Proc. Natl. Acad. Sci. 98, 10011–10016.
Mardia, K.V., Bookstein, F., Moreton, I.J., 2000. Statistical assessment of bilateral symmetry of shapes. Biometrika 87, 285–300.
McCown, T., Keith, A., 1939. The Stone Age of Mount Carmel. In: The Fossil Human Remains from the Levallois-Mousterian, vol. 2. Clarendon, Oxford.
Mercier, N., Valladas, H., 2003. Reassessment of TL age estimates of burnt flints from the Paleolithic site of Tabun Cave. Israel. J. Hum. Evol. 45, 401–409.
Mercier, N., Valladas, H., Valladas, G., Reyss, J.L., Jelinek, A., Meignen, L., Joron, J.L., 1995. TL dates of burnt flints from Jelinek's excavations at Tabun and their implications. J. Archaeol. Sci. 22, 495–509.
Mitteroecker, P., Bookstein, F.L., 2011. Linear discrimination, ordination, and the visualization of selection gradients in modern morphometrics. Evol. Biol. 38, 100–114.
Mitteroecker, P., Gunz, P., 2009. Advances in geometric morphometrics. Evol. Biol. 36, 235–247.
Mitteroecker, P., Gunz, P., Bernhard, M., Schaefer, K., Bookstein, F.L., 2004. Comparison of cranial ontogenetic trajectories among great apes and humans. J. Hum. Evol. 46, 679–697.
Mounier, A., Marchal, F., Condemi, S., 2009. Is *Homo heidelbergensis* a distinct species? New insight on the Mauer mandible. J. Hum. Evol. 56, 219–246.
Mounier, A., Condemi, S., Manzi, G., 2011. The stem species of our species: a place for the archaic human cranium from Ceprano, Italy. PLoS One 6, e18821.
Muttoni, G., Scardia, G., Kent, D.V., Swisher, C.C., Manzi, G., 2009. Pleistocene magnetochronology of early hominin sites at Ceprano and Fontana Ranuccio, Italy. Earth Planet. Sci. Lett. 286, 255–268.
Potts, R., Behrensmeyer, A.K., Deino, A., Ditchfield, P., Clark, J., 2004. Small mid-Pleistocene hominin associated with East African Acheulean technology. Science 305, 75–78.
R Development Core Team, 2010. R: A Language and Environment for Statistical Computing. R Foundation for Statistical Computing.
Relethford, J.H., 1994. Craniometric variation among modern human populations. Am. J. Phys. Anthropol. 95, 53–62.
Relethford, J.H., 2004a. Boas and beyond: migration and craniometric variation. Am. J. Hum. Biol. 16, 379–386.
Relethford, J.H., 2004b. Global patterns of isolation by distance based on genetic and morphological data. Hum. Biol. 76, 499–513.
Rightmire, G.P., 1998a. Evidence from facial morphology for similarity of Asian and African representatives of *Homo erectus*. Am. J. Phys. Anthropol. 106, 61–85.
Rightmire, G.P., 1998b. Human evolution in the Middle Pleistocene: the role of *Homo heidelbergensis*. Evol. Anthropol. 6, 218–227.
Rightmire, G.P., 2001. Morphological diversity in Middle Pleistocene Homo. In: Wood, B., Tobias, P.V. (Eds.), Humanity from African Naissance to Coming Millenia: Colloquia in Human Biology and Paleoanthropology. Firenze University Press, Firenze, pp. 135–140.
Rightmire, G.P., 2007. Later Middle Pleistocene *Homo*. In: Henke, W., Tattersall, I. (Eds.), Handbook of Paleoanthropology. Springer, Heidelberg, pp. 1695–1715.
Rightmire, G.P., 2008. *Homo* in the Middle Pleistocene: hypodigms, variation, and species recognition. Evol. Anthropol. 17, 8–21.
Rightmire, G.P., 2009. Out of Africa: modern human origins special feature: Middle and Later Pleistocene hominins in Africa and Southwest Asia. Proc. Natl. Acad. Sci., 16046–16050.
Rink, W.J., Schwarcz, H.P., 1995. ESR ages for Krapina hominids. Nature 378, 24.
Rink, W.J., Schwarz, H.P., Lee, H.K., Rees-Jones, J., Rabinovich, R., Hovers, E., 2001. Electron spin resonance (ESR) and thermal ionization mass spectrometric (TIMS) $^{230}Th/^{234}U$ dating of teeth in Middle Paleolithic layers at Amud Cave, Israel. Geoarchaeology 16, 701–717.
Rohlf, F.J., 1993. Relative warp analysis and an example of its application to mosquito wings. In: Marcus, L.F., Bello, E., García-Valdecasas, A. (Eds.), Contributions to morphometrics. Museo Nacional de Ciencies Naturales, Madrid, pp. 131–159.
Roseman, C.C., 2004. Detecting interregionally diversifying natural selection on modern human cranial form by using matched molecular and morphometric data. Proc. Natl. Acad. Sci. 101, 12824–12829.
Roseman, C.C., Weaver, T.D., 2007. Molecules versus morphology? Not for the human cranium. Bioessays 29, 1185–1188.
Schillaci, M.A., 2008. Human cranial diversity and evidence for an ancient lineage of modern humans. J. Hum. Evol. 54, 814–826.
Schwarcz, H.P., Bietti, A., Buhay, W.M., Stiner, M.C., Grün, R., Segre, A., 1991. On the reexamination of Grotta Guattari: uranium-series and electron-spin-resonance dates. Curr. Anthropol. 32, 313–316.
Shen, G., Gao, X., Gao, B., Granger, D.E., 2009. Age of Zhoukoudian *Homo erectus* determined with (26)Al/(10)Be burial dating. Nature 458, 198–200.
Shen, G., Wang, W., Wang, Q., Zhao, J., Collerson, K., Zhou, C., Tobias, P.V., 2002. U-Series dating of Liujiang hominid site in Guangxi, Southern China. J. Hum. Evol. 43, 817–829.
Simmons, T., Falsetti, A.B., Smith, F.H., 1991. Frontal bone morphometrics of southwest Asian Pleistocene hominids. J. Hum. Evol. 20, 249–269.
Skelton, R.R., McHenry, H.M., 1992. Evolutionary relationships among early hominids. J. Hum. Evol. 23, 309–349.
Skinner, M.M., Wood, B.A., Boesch, C., Olejniczak, A.J., Rosas, A., Smith, T.M., Hublin, J.J., 2008. Dental trait expression at the enamel-dentine junction of lower molars in extant and fossil hominoids. J. Hum. Evol. 54, 173–186.
Slice, D.E., 2005. Modern Morphometrics in Physical Anthropology. Kluwer Academic, New York.
Smith, F.H., Falsetti, A.B., Donnelly, S.M., 1989. Modern human origins. Am. J. Phys. Anthropol. 32, 35–68.
Smith, F.H., Janković, I., Karavanic, I., 2005. The assimilation model, modern human origins in Europe, and the extinction of Neandertals. Quatern. Int. 137, 7–19.
Smith, F.H., 1982. Upper Pleistocene hominid evolution in South-Central Europe: a review of the evidence and analysis of trends. Curr. Anthropol. 23, 667–703.
Smith, F.H., 1992. Models and realities in modern human origins: the African fossil evidence. Phil. Trans. R. Soc. Lond 337, 243–250.
Smith, H.F., 2009. Which cranial regions reflect molecular distances reliably in humans? Evidence from three-dimensional morphology. Am. J. Hum. Biol. 21, 36–47.
Smith, T.M., Tafforeau, P., Reid, D.J., Grün, R., Eggins, S., Boutakiout, M., Hublin, J.-J., 2007. Earliest evidence of modern human life history in North African early *Homo* sapiens. Proc. Natl. Acad. Sci. 104, 6128–6133.
Sohn, S., Wolpoff, M.H., 1993. Zuttiyeh face: a view from the east. Am. J. Phys. Anthropol. 91, 325–347.
Stansfield Nee Bulygina, E., Gunz, P., 2011. Skhodnya, Khvalynsk, Satanay, and Podkumok Calvaria: possible upper paleolithic hominins from European Russia. J. Hum. Evol. 60, 129–144.
Street, M., 2002. Ein Wiedersehen mit dem Hund von Bonn-Oberkassel. Bonn. Zool. Beitr 50, 269–290.
Stringer, C.B., 1974. Population relationships of later Pleistocene hominids: a multivariate study of available crania. J. Archaeol. Sci. 1, 317–342.
Stringer, C.B., 1983. Some further notes on the morphology and dating of the Petralona hominid. J. Hum. Evol. 12, 731–742.
Stringer, C.B., 2002. Modern human origins: progress and prospects. Phil. Trans. R. Soc. Lond. 357, 563–579.
Suzuki, H., Takai, F., 1970. The Amud Man and His Cave Site. University of Tokyo Press, Tokyo.
Trinkaus, E., 1982. Cranial deformation in the Shanidar 1 and 5 Neandertals. Curr. Anthropol 23, 198–199.
Trinkaus, E., 1983. The Shanidar Neandertals. Academic Press, New York.
Trinkaus, E., 1989. Issues concerning human emergence in the later Pleistocene. In: Trinkaus, E. (Ed.), The Emergence of Modern Humans: Biological Adaptations in the Later Pleistocene. Cambridge University Press, Cambridge, pp. 1–17.
Trinkaus, E., 2005. Early modern humans. Ann. Rev. Anthropol. 34, 207.
Trinkaus, E., 2007. European early modern humans and the fate of the Neandertals. Proc. Natl. Acad. Sci. 104, 7367–7372.
Turville-Pétre, F., 1927. Researches in Prehistoric Galilee, 1925-26. Council of the British School of Archaeology in Jerusalem, London.
van Vark, G.N., 1995. The study of hominid skeletal remains by means of statistical methods. In: Boas, N.T., Wolfe, G.D. (Eds.), Biological Anthropology: The State of the Science. Oregon State University Press, Corvallis, pp. 71–90.
Vandermeersch, B., 1981. Les hommes fossiles de Qafzeh (Israël). Editions du Centre national de la recherche scientifique, Paris.
Vandermeersch, B., 1989. The evolution of modern humans: recent evidence from southwest Asia. In: Mellars, P.A., Stringer, C. (Eds.), The Human Revolution. Edinburgh University Press, Edinburgh, pp. 155–164.
von Cramon-Taubadel, N., 2009. Congruence of individual cranial bone morphology and neutral molecular affinity patterns in modern humans. Am. J. Phys. Anthropol. 140, 205–215.

von Cramon-Taubadel, N., Lycett, S.J., 2008. Brief communication: human cranial variation fits iterative founder effect model with African origin. Am. J. Phys. Anthropol. 136, 108–113.
Wall, J.D., Lohmueller, K.E., Plagnol, V., 2009. Detecting ancient admixture and estimating demographic parameters in multiple human populations. Mol. Biol. Evol. 26, 1823–1827.
Weaver, T.D., 2009. The meaning of Neandertal skeletal morphology. Proc. Natl. Acad. Sci. 106, 16028.
Weaver, T.D., Roseman, C.C., Stringer, C.B., 2007. Were Neandertal and modern human cranial differences produced by natural selection or genetic drift? J. Hum. Evol. 53, 135–145.
Weber, G.W., Gunz, P., Mitteroecker, P., Stadlmayr, A., Bookstein, F.L., Seidler, H., 2006. External geometry of Mladeč neurocrania compared with anatomically modern humans and Neandertals. In: Teschler-Nicola, M. (Ed.), Early Modern Humans at the Moravian Gate: Mladeč Caves and Their Remains. Springer, Heidelberg, pp. 453–471.
Weidenreich, F., 1943. The Skull of Sinanthropus Pekinensis: A Comparative Study on a Primitive Hominid Skull. Geological Survey of China, Pehpei, Chungking.
Wiley, D.F., Amenta, N., Alcantara, D.A., Deboshmita, G., Kil, Y.J., Delson, E., Harcourt-Smith, W., Rohlf, F.J., St John, K., Hamann, B., 2005. Evolutionary morphing. Proc. IEEE Visualizations, 431–438.
Wolpoff, M.H., Xinzhi, Wu, Thorne, A.G., 1984. Modern Homo sapiens origins: a general theory of hominid evolution involving the fossil evidence from East Asia. In: Smith, F.H., Spencer, F. (Eds.), The Origins of Modern Humans: A World Survey of the Fossil Evidence. Alan R. Liss, New York, pp. 411–483.
Wood, B., Lieberman, D.E., 2001. Craniodental variation in *Paranthropus boisei*: a developmental and functional perspective. Am. J. Phys. Anthropol. 116, 13–25.
Woodward, A.S., 1921. A new cave man from Rhodesia, South Africa. Nature 108, 371–372.
Zeitoun, V., 2001. The taxinomical position of the skull of Zuttiyeh. C. R. Acad. Sci. 332, 521–525. Paris.